Accepted Manuscript

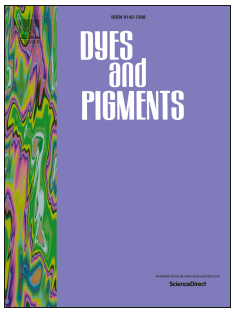

A lysosomal probe for monitoring of pH in living cells and ovarian tumour

Bo Li, Guang bo Ge, Lanlan Wen, Ye Yuan, Ran Zhang, Xiaojun Peng, Fengyu Liu, Shiguo Sun

PII: S0143-7208(16)31105-6

DOI: 10.1016/j.dyepig.2016.12.043

Reference: DYPI 5668

To appear in: *Dyes and Pigments*

Received Date: 3 November 2016

Revised Date: 18 December 2016

Accepted Date: 19 December 2016

Please cite this article as: Li B, Ge Gb, Wen L, Yuan Y, Zhang R, Peng X, Liu F, Sun S, A lysosomal probe for monitoring of pH in living cells and ovarian tumour, *Dyes and Pigments* (2017), doi: 10.1016/j.dyepig.2016.12.043.

A lysosomal probe for monitoring of pH in living cells and ovarian tumour

Bo Li[a,1], Guang bo Ge[b,1], Lanlan Wen[a,1], Ye Yuan[a], Ran Zhang[a], Xiaojun Peng[a], Fengyu Liu[a,*] and Shiguo Sun[c,*]

[a] *State Key Laboratory of Fine Chemicals, School of Chemistry, Dalian University of Technology, No. 2, Linggong Road, Ganjingzi District, 116023 Dalian, China.*
[b] *Dalian Institute of Chemical Physics, Chinese Academy of Sciences, Dalian 116023, China.*
[c] *Key Laboratory of Xinjiang Endemic Phytomedicine Resources, Ministry of Education, School of Pharmacy, Shihezi University, Shihezi 832000, China*
[1] *These authors contributed equally to this work.*

ABSTRACT

Intracellular pH is important in regulating various cellular behaviour and pathological conditions. We synthesised a rhodamine-based lysosomal pH probe (hereafter referred to as RD) with a pKa of 4.10. The probe exhibited favourable “on-off” reversibility between pH 3.25 and 7.20 for at least five cycles. RD can be employed to distinguish cancer cells from normal cells on the basis of different fluorescence response. RD performed well in the detection of lysosomal pH induced by artesunate, chloroquine and dexamethasone in MCF-7 cells. The intense fluorescence of RD in ovarian tumour indicated the higher acidity in tumour tissues than that in normal tissues. Furthermore, RD worked well in the imaging of excised mouse stomach and living mice under acidic stimulation. These data demonstrate the applicability of RD in monitoring pH in complex biological systems.

Key words : monitoring pH, lysosome, fluorescent probe, cells, ovarian tumour

1. Introduction

Lysosome is an acidic organelle in all eukaryotic cells excluding erythrocytes [1], which plays significant roles in many physiological activities, including maintaining cholesterol homeostasis, repairing damaged cytoplasmic membrane, restoring bone and tissue and defending against pathogens [2]. It is noted that lysosomal pH is

closely related to its function [3, 4]. Malfunction of lysosomes can cause many diseases, such as cancer, gout and neurodegenerative diseases [5]. Therefore, imaging of lysosomes and monitoring of pH status is important.

To date, there are several methods had been developed to detect pH in vitro or vivo, such as weak acid and base distribution [6], nuclear magnetic resonance spectroscopy [7], microelectrodes [8], and fluorescent probes [9]. Compared with other techniques, fluorescence detection using small molecular probes, has regarded as a promising method in living cells due to its sensitivity, selectivity, simple operation, and especially nondestructive characteristics. Some efforts have been directed toward the development of fluorescent pH sensors [10-15], especially lysosomal pH sensors [2, 16-24]. For instance, Li [2] constructed a pH sensitive probe based on a 4-acylated naphthalimide, Peng [16] synthesised a pH sensor by introducing a novel lysosomal location group, Yu [17] developed two rhodamine-based pH probes via the click reaction, Zhang [18] reported arhodamine-based pH probe, Zhao [19] exploited a rhodamine B-based lysosomal pH probe, Liu [20] constructed three lysosomal pH probes based on piperazine-modified BODIPY dyes and Wang [21] designed a pH-activatable near-infrared (NIR) probe through combining a cyclic boronate with Si-rhodamine. Some ratiometric fluorescent probes have been developed for tracking lysosomal pH in vivo. Zhang [22] reported a new lysosome-targeted ratiometric fluorescent probe by hybridizing morpholine with a xanthane derivative and an o-hydroxybenzoxazole group, Zhao [23] reported a ratiometric lysosomal pH probe based on the naphthalimide–rhodamine. Very recently, Lin [24] developed a novel dual site-controlled and lysosome-targeted ratiometric fluorescent probe based on coumarin and naphthalimide fluorophores. These probes showed general suitability of specific labelling of acidic lysosomes and tracking their pH in living cells. However, not much fluorescence difference can be observed in the case of normal and cancer cells for these probes. A pyridineium-2-yl Darrow Red analogue with a pKa of 2.4 was adopted for the selective detection of cancer cells [25]. Unfortunately, the status of normal cells cannot be visualised because of the absence of emission when the pH exceeds 4.0. Cancer cells contain rich hydrogen ions [26], and the acidity of

lysosomes in cancer cells is lower than that in normal cells [25]. A probe which can work well both in cancer and normal cells, and which can easily distinguish different cells on the basis of fluorescence response is highly desirable.

Low extracellular pH is a symbol of solid tumours [27]. This acidity mainly arises from high lactic acid production due to enhanced glycolysis [28]. As a product of aerobic respiration in vivo, CO_2 may be another significant source of acidification of tumour interstitium [29]. Some probes were reported for monitoring of tumour pH. For instance, Kobayashi [30] designed four novel acidic pH–activatable probes by conjugating the boron-dipyrromethene fluorophore with a cancer-targeting monoclonal antibody. The next year, the group reported a dual-controlled activation fluorescent imaging probe through combining pH-sensitive fluorophore pHrodo or TAMRA with the cancer targeting molecules avidin and trastuzumab [31]. Shirmanova [32] used the novel genetically encoded indicator SypHer2 for pH mapping in living cancer cells in vitro and in tumors in vivo. Achilefu [33] developed a highly tumour-selective probe with a pKa of 4.7 to image acidic cell organelles and detect primary and metastatic cancer. This professor introduced a cyclic arginine-glycine-aspartic acid (cRGD) peptide to a Cy7 molecule to target $R_v\beta_3$ integrin (ABIR), which is highly overexpressed during tumour angiogenesis. In 2015, Prof. Achilefu [34] found that the Cy7 molecule alone can detect tumour through electrostatic changes produced by the extracellular acidic pH environment of diverse solid tumors without tumor targeted groups. Thus, it inspires us to develop a single molecule probe which can not only distinguish cancer cells from normal cells but also detect tumours.

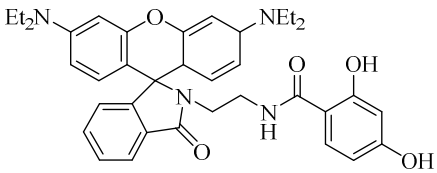

Scheme 1. Structure of Probe RD

Rhodamine dye, which features a spirocyclic structure, is an ideal OFF-ON fluorescence switch candidate. In general, there are no fluorescence at basic and

neutral pH because of the ‘‘ring-closed’’ state of spirocyclic structure. When the H^+ increases within a certain range, the ring is open, leading to a significant fluorescence enhancement [16, 35]. Accordingly, we developed a probe termed RD (Scheme 1) by introducing 2, 4-dihydroxybenzoic acid to rhodamine B. RD, which features a pKa of 4.1, facilitates remarkable fluorescence intensity enhancement and significant colour variation from colourless to pink when the pH is adjusted from 7.02 to 3.06. RD performed well in the monitoring of lysosomal pH induced by artesunate (ART), chloroquine and dexamethasone. The intense fluorescence of RD in ovarian tumour indicated the higher acidity in tumour tissues than that in normal tissues. Furthermore, RD worked well in the imaging of excised mouse stomach and living mice under acidic stimulation.

2. Materials and methods

2.1 Materials and instruments

All solvents and reagents used were reagent grade and used without further purification unless otherwise stated. The solution of RD was dissolved in DMSO at a concentration of 1 mM as the stock solution and stored in a refrigerator (2 ºC) for use. B-R-E (Britton-Robinson buffer/EtOH, v/v = 5 : 5) solution was mixed by 40 mM acetic acid, boric acid, and phosphoric acid [36]. Sodium hydroxide (0.1 M) was utilized for tuning pH values of B-R-E solution. The solution of metal ions was prepared from nitrate salts. Deionized water was used throughout the experiment. Cells were purchased from Institute of Basic Medical Sciences (IBMS) of the Chinese Academy of Medical Sciences.

NMR spectra were recorded on a VARIAN INOVA 400 (or a Bruker Avance II 400 MHz) spectrometer. Chemical shifts (δ) were reported as ppm (in $CDCl_3$ or DMSO-d_6, with TMS as the internal standard). Fluorescence spectra were performed on a VAEIAN CARY Eclipse fluorescence spectrophotometer (Serial No. FL0812:M018). Excitation and emission slit widths were modified to adjust the fluorescence intensity to a suitable range. Absorption spectra were measured on a Perkin Elmer Lambda 35

UV/VIS spectrophotometer (Perkin Elmer). Mass spectrometric data were achieved with HP1100LC/MSD MS and an LC/Q-TOF-MS instruments. Imaging in vivo mice was performed using a Night OWL II LB 983 system equipped with an NC 100 CCD deep-cooled camera (Berthold Technologies, Bad Wildbad, Germany). All pH measurements were performed using a Model PHS-3C meter. Flash column chromatography was performed using silica gel (100-200 mesh) obtained from Qingdao Ocean Chemicals. Lyso Tracker Green was purchased from Life Technologies Co. (USA).

2.2 Synthesis of compound RD

RD was synthesised by two procedures (Scheme S1). The first step, RB (2.51 g, 5.2 mmol) was dissolved in ethanol (50 mL), then 5 mL ethylenediamine was added in dropwise to the flask and the reaction mixture was stirred at 90ºC for 8 h. After the solution was cooled to room temperature, the solution was concentrated under reduced pressure and the residue was purified by column chromatography (DCM : MeOH = 10 : 1, v/v) to afford a light yellow solid R2 in 75% yield. ^{1}H NMR (400 MHz, $CDCl_3$), δ 7.89 (m, 1H), 7.60-7.33 (m, 2H), 7.18-7.00 (m, 1H), 6.58-6.12 (m, 6H), 3.50-3.23 (m, 8H), 3.23 (t, J = 6.6 Hz, 2H), 2.45 (t, J = 6.6 Hz, 2H), 1.17 (t, J = 7.0 Hz, 12H). MS: $(M+H)^+$, calcd: m/z = 485.29, found: m/z = 485.27.

The second step, 2,4-dihyoxybenzoicacid (308 mg, 2 mmol) was dissolved in acetonitrile (20 mL), then 1-(3-Dimethylaminopropyl)-3-ethylcarbodiimide hydrochloride (EDCI, 384 mg, 2 mmol) and 4-dimethylaminopyridine (DMAP, drops) were added into the flask and the reaction mixture was stirred at room temperature for 1 h. After, R2 (500 mg, 1 mmol) was added to the flask and the reaction mixture was stirred at 90 ºC for 12 h. After cooled down to room temperature, the solution was concentrated under reduced pressure and the residue was purified by column chromatography (DCM : MeOH = 30 : 1, v/v) to afford a white solid RD in 65% yield. ^{1}H NMR (400 MHz, $CDCl_3$) , δ 12.91 (s, 1H), 8.31 (s, 1H), 7.93 (dd, J = 6.0, 2.4 Hz, 1H), 7.58 (d, J = 8.7 Hz, 1H), 7.55-7.40 (m, 2H), 7.11 (dd, J = 5.9, 2.1 Hz, 1H), 6.62-6.16 (m, 8H), 3.63-3.03 (m, 12H), 1.17 (t, J = 7.1 Hz, 12H). ^{13}C NMR (100 MHz,

$CDCl_3$), δ 171.68, 170.72, 164.37, 162.66, 154.38, 153.84, 149.65, 133.76, 130.41, 129.02, 128.83, 128.46, 124.51, 123.70, 109.02, 107.94, 107.58, 104.53, 104.49, 98.29, 67.03, 46.38, 44.91, 41.89, 39.75, 13.10. HRMS: $(M+H)^+$, calcd: *m/z* = 621.3071, found: *m/z* = 621.3067.

2.3 Fluorescence detection

Absorption and emission spectra were primarily measured in B-R-E solution. The resulting solution was equilibrated for 15 min before measurement. The fluorescence spectra were measured with excitation wavelength at 540 nm.

Photo-bleaching experiments were performed according to the literature [37]. Concentration of RD and commercialized dye Lyso Tracker Green were 10 μM, at pH 4.25, 500 W halogen lamp as light source, saturated $NaNO_2$ (50 g/L) solution as a light filter (to cut off light of wavelength under 400 nm) and hot filters, keep light source and the test samples at 30 cm distance respectively and record the fluorescence intensity of probe RD and Lyso Tracker Green, and processing the biggest fluorescence intensity values normalized.

2.4 Live cell imaging experiments

Cells were cultured in Dulbecco's modified Eagle's medium (DMEM, Invitrogen) supplemented with 10% fetal bovine serum (Invitrogen). The cells were seeded in 24-well flat-bottomed plates and then incubated for 24 h at 37ºC under 5% CO_2. Before imaging, the live cells were incubated with RD (5 μM) for different time and then washed with phosphate-buffered saline (PBS) three times. Fluorescence imaging was performed using an OLYMPUSFV-1000 inverted fluorescence microscope with a 60 × objective lens. Under the confocal fluorescence microscope, RD was excited at 559 nm and emission was collected at 565-620 nm. For the detection of Lysosomal pH, MCF-7 cells were incubated with RD (5 μM) at 37 ºC for 1 h and then artesunate (ART, 50 μM), chloroquine (20 μM), dexamethasone (100 μM) were added respectively to incubate with cells at 37 ºC for different time.

2.5 MTT assay

Measurement of cell viability was evaluated by reducing of MTT (3-(4, 5)-dimethylthiahiazo(-2-yl)-3,5-diphenytetrazoliumromide) to formazan crystals using mitochondrial dehydrogenases (Mosmann, 1983). HepG-2 cells were seeded in 96-well microplates (Nunc, Denmark) at a density of 1×10^5 cells/mL in 100 mL medium containing 10% fetal bovine serum (FBS, invitrogen). After 24 h of cell attachment, the plates were washed with 100 μL/well PBS. The cells were then cultured in medium with 0.5, 1, 2 and 5 μM of RD for 12 h. Cells in culture medium without RD were used as the control. Six replicate wells were used for each control and test concentration10 μL of MTT (5 mg/mL) prepared in PBS was added to each well and the plates were incubated at 37 ºC for another 4 h in a 5% CO_2 humidified incubator. The medium was then carefully removed, and the purple crystals were lysed in 200 μL DMSO. Optical density was determined on a microplate reader (Thermo Fisher Scientific) at 570 nm (OD) with subtraction of the absorbance of the cell-free blank volume at 630 nm (OD_K). Cell viability was expressed as a percent of the control culture value, and it was calculated using the following equation [38]:Cells viability (%) = $(OD_{dye}- OD_{Kdye})/ (OD_{control}- OD_{Kcontrol}) \times 100$.

2.6 Animal Models and in Vivo Animal Studies

All animal experiments were performed in compliance with the Guiding Principles for the Care and Use of Laboratory Animals, Dalian Medical College, China. Before animal imaging and analysis, SPF (Specific pathogen Free) Kunming mice (7-week-old, 20-25 g) were starved 12 h because of possible food fluorescence interference at the emission wavelength of the fluorescent dyes. The experiments were performed using a Night OWL II LB 983 system equipped with an NC 100 CCD deep-cooled camera (Berthold Technologies, Bad Wildbad, Germany), with an excitation filter of 530 nm and an emission filter of 600 ± 20 nm.

3. Results and discussion

3.1 Design and synthesis of RD

RD was readily synthesised by a two-step procedure (Scheme S1) and confirmed by ^{1}H NMR, ^{13}C NMR and HRMS spectra (Fig. S1-S5). The proposed sensing mechanism of RD for H^{+} is shown in Scheme S2. To provide evidence, the change between RD and the protonated form RDH was characterized through ^{1}H NMR titration (Fig. S6). The addition of trifluoroacetic acid led to the ‘‘ring-opened’’ state of spirocyclic structure RDH. Hence, a down-field shift can be observed for eight protons of NEt_2 and six protons of benzene ring in RB. After the addition of NaOH, the spirocyclic ring was closed, and the corresponding proton shift was recovered.

3.2 Spectroscopic properties and optical responses to pH

The spectroscopic properties of RD were initially determined in a B-R-E solution. As expected, the fluorescence intensity reached saturation within 15 min at pH 4.25 (Fig. S7a). As shown in Fig. 1a, the absorption spectra of RD in weak basic aqueous solution (pH 7.02) displayed almost no absorption bands at 500–600 nm. The changes of pH from 7.02 to 3.06 caused a gradual increase of the absorbance at 564 nm, indicating that the spirolactam ring of rhodamine was opened. Moreover, the solution changed from colourless to pink, which was visible by the naked-eye. The pH response of RD is displayed in Fig. 1b. RD was non-fluorescent under neutral conditions because of its “ring-closed” form. However, as the pH decreased from 7.02 to 3.06, a remarkable enhanced fluorescence signal appeared at 586 nm because of spirocyclic ring opening. The fluorescence spectra of RD was obtained under pH 3.26 in Fig. S7b.

A good linearity (R^2 = 0.9867) between fluorescence intensity and pH (3.46-5.06) was obtained by fluorescence titration (Fig. 2a). With fluorescence intensity (at 586 nm) as a function of pH, a pKa of 4.10 was calculated using the Henderson-Hasselbalch equation [39], suggesting that RD may detect pH for acidic organelles such as lysosomes in vivo. Furthermore, the reversibility of the probe in the B-R-E solution was studied between pH 3.25 and 7.20 (Fig. 2b). Approximately 94% of the original signal was successfully restored after five cycles, providing a

possibility for monitoring pH change repeated. The fluorescence quantum yield of RD at pH 3.26 was determined to be 0.475 [40].

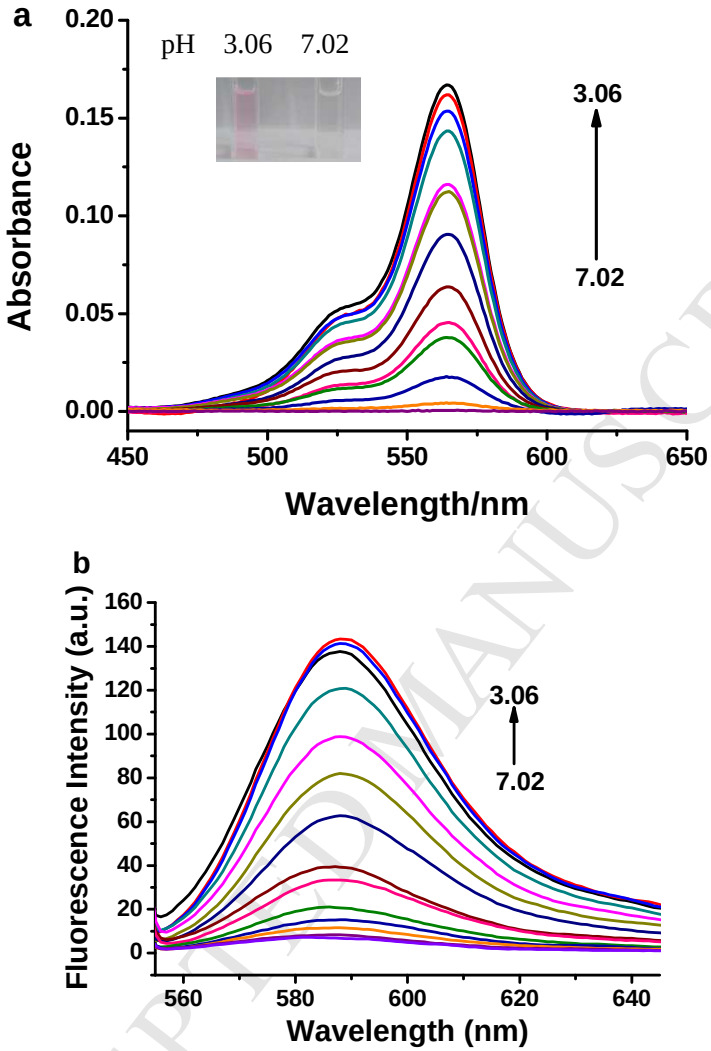

Fig. 1 (a) Absorption and (b) fluorescence spectra (λ_{ex} = 540 nm) of RD (10 μM) in B-R-E solution with different pH 7.02, 6.06, 5.26, 4.86, 4.66, 4.46, 4.26, 4.06, 3.86, 3.66, 3.46, 3.26 and 3.06.

Nitrogen atom can bind with many metal ions, such as Pd^{2+} and Cu^{2+} in solution, and the binding may cause ring-opening in rhodamine-based probes [41, 42]. Thus, investigating whether other ions are potential interferents is necessary [43]. As shown in Fig. S8a, RD did not exhibit any observable fluorescence change in the presence of common cations, such as Na^{+}, K^{+}, Cr^{3+}, Ag^{+}, Cu^{2+}, Cd^{2+}, Hg^{2+}, Fe^{3+}, Pb^{2+}, Ni^{2+}, Co^{2+}, Fe^{2+}, Zn^{2+}, Ca^{2+}, Mg^{2+}, $Mn^{2+}$and Al^{3+} at pH 7.02. While significant fluorescence enhancement occurred in the case of pH 4.25 as shown in Fig. S8b. The high

selectivity of RD over interfering species along with the above-mentioned excellent reversibility indicates that RD demonstrates a significant potential as a pH probe for practical applications.

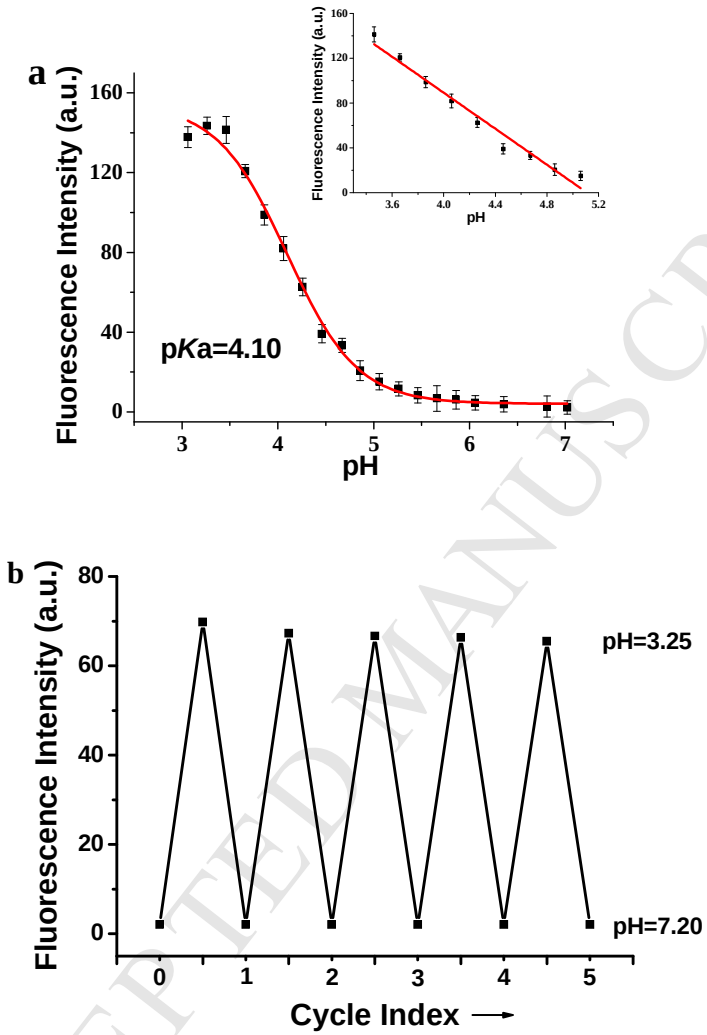

Fig. 2 (a) Sigmoidal fitting of the pH-dependent fluorescence intensity at 586 nm of RD (10 μM) in B-R-E solution, with different pH 7.02, 6.81, 6.36, 6.06, 5.86, 5.66, 5.46, 5.26, 5.06, 4.86, 4.66, 4.46, 4.26, 4.06, 3.86, 3.66, 3.46, 3.26 and 3.06. Inset: the good linearity in the pH range of 3.46-5.06, (b) The reversibility of the probe RD (10 μM) between pH 3.25 and 7.20 in B-R-E solution. Fluorescence intensity change of RD at 586 nm along with the addition of HCl (1 M) and NaOH (1 M) to the solution for five times, respectively (λ_{ex} = 540 nm).

3.3 Fluorescence imaging and distribution in living cells

To evaluate the cell membrane permeability of RD, imaging was monitored in the red channel (565-620 nm) with a 559 nm laser under a confocal laser scanning microscope. As shown in Fig. S9, the probe can stain the MCF-7 cell in 10 min,

demonstrating its good membrane permeability. After 30 min, the staining can be finished and focused mainly in the cytoplasm.

To study the subcellular distribution of RD, we used commercial Lyso Tracker Green to co-stain with the probe (Fig. 3). After incubating with 5 μM RD for 30 min, MCF-7 cells were further stained with 1 μM Lyso Tracker Green for 10 min. A co-localisation coefficient (Pearson's correlation) of 0.90 can be reached between the red emission of RD and the green emission of Lyso Tracker Green. HeLa and HepG-2 cells were also tested with higher Pearson's correlations of 0.98 and 0.94, respectively (Fig. S10 and S11).

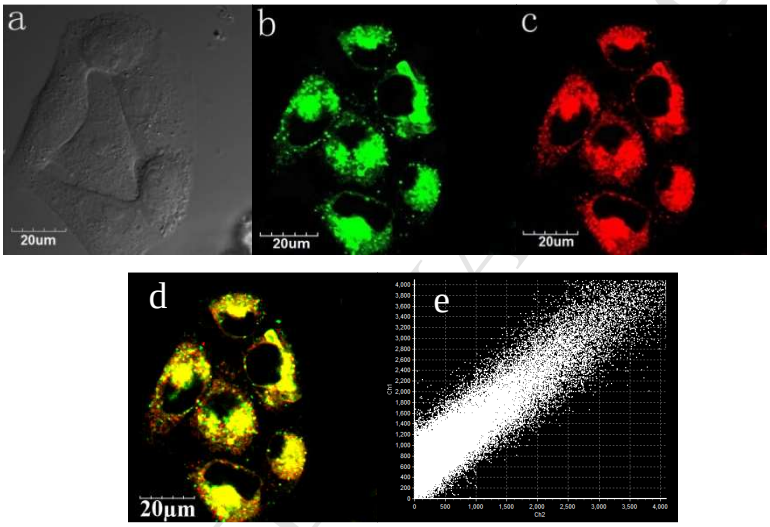

Fig. 3 Co-localization experiments of MCF-7 cells incubated with RD (5 μM) for 30 min and then incubated with Lyso Tracker Green (1.0 μM) for 10 min at 37 ºC under 5% CO_2. (a) Bright image, (b) Confocal image from LysoTracker Green on green channel (λ_{ex} = 488 nm), (c) Confocal image from RD on red channel (λ_{ex} = 559 nm), (d) Merged image of b and c, (e) Correlation plot of the intensities of RD and Lyso Tracker Green (Rr = 0.90).

Furthermore, confocal fluorescent imaging was performed in Human hepatoma carcinoma cells (HepG-2) and Human normal liver cells (HL-7702) using RD. Probe RD gave very strong red emission in HepG-2 cells (Fig. S11), while only slightly weaker emission was observed in HL-7702 cells (Fig S12g-i). To provide further evidence, normal cells (COS-7, BEAS-2B) and cancer cell lines (MCF-7, HeLa) were used to repeat imaging. The results indicate that for normal cells, such as COS-7,

BEAS-2B and HL-7702, only weak emission was found after incubation for 60 (Fig. S12) and 120 min (Fig. S13), while, intense red emission can be observed for the above mentioned cancer cells in 30 min (Fig. 3, S10 and S11). This result demonstrates that the lysosomal pH in cancer cells is lower than that in normal cells as reported [25]. The different fluorescence responses of RD can be employed to separate cancer cells from normal cells.

The cytotoxicity of RD was evaluated using MTT assay (Fig. S14). Negligible toxicity existed under 5 μM. Especially, RD exhibited higher photostability than commercial Lyso Tracker Green at pH 4.25 (Fig. S15). The fluorescence intensity of RD only decreased to 94% after irradiation under a 500 W halogen lamp for 4 h, whereas that of Lyso Tracker Green significantly decreased to 54%. This result demonstrates the higher photostability of RD than Lyso Tracker Green. Thus, RD may be used for long-term monitoring of pH in the future.

3.4 Monitoring lysosomal pH in cells

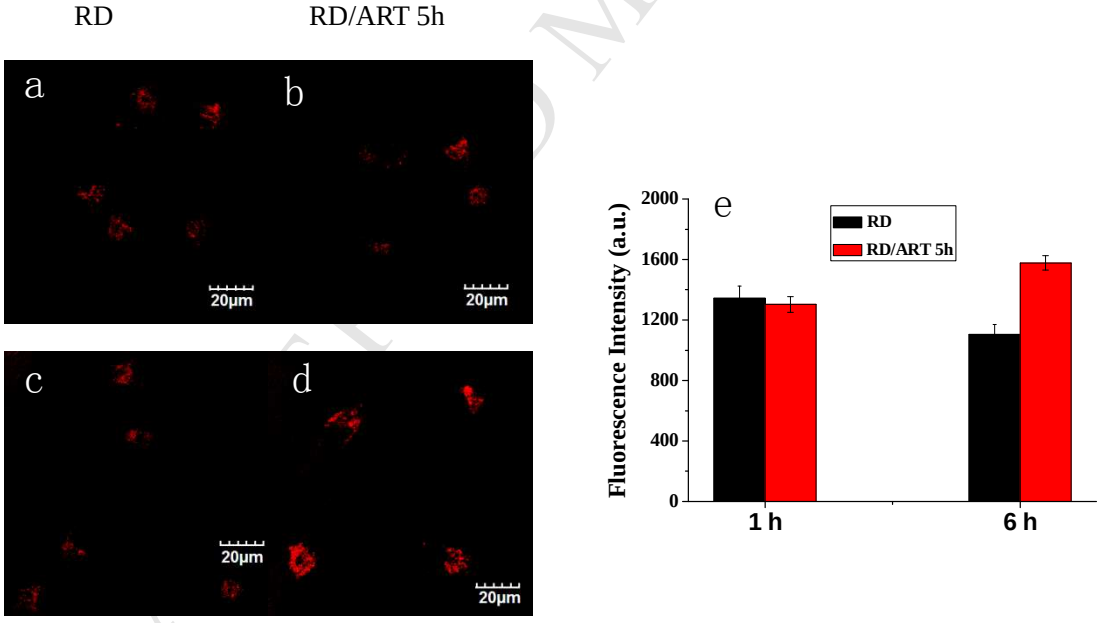

Fig. 4 Confocal images of RD (5.0 μM) in MCF-7 cells. (a, b) RD incubated with cells for 1 h, (c) RD incubated with cells for 6 h, (d) Incubated with RD for 1 h then exposed to 50 μM ART for 5 h, (e*) Quantification of fluorescence intensity from RD and RD/ART. Scale bar: 20 μm, λ_{ex} = 559 nm, λ_{em} = 565-620 nm. (*: The values obtained were averaged from six arbitrarily fluorescent areas in a, b, c, d image.)

Artesunate (ART) [44], a water-soluble derivative of artemisinin, has been widely used to cure malaria. It preferably accumulates in the lysosomes and decreases lysosomal pH in a time-dependent manner [45]. Thus, ART-induced lysosomal pH changes were studied on RD-stained MCF-7 cells (Fig. 4). To compare the intensity on amounts, six arbitrarily fluorescent areas in every image were chosen to represent the lysosomal regions of the MCF-7 cells. The values obtained were subsequently averaged for each case (Fig. 4e) [16]. After treatment with 50 μM ART for 5 h, RD exhibited a stronger red fluorescence compared with the control. To provide further evidence (Fig. S16), chloroquine [46] was also used to induce lysosomal pH changes as reported in the literature [47, 48]. However, chloroquine led to the alkalisation of the lysosome, and this effect was opposite to that of ART. Compared with the fluorescence intensity in the cells only stained with RD, that in the cells stained with RD and chloroquine significantly reduced. These results indicate that RD can be a lysosomal pH-responsive sensor in cell biology.

Dexamethasone is a chemotherapeutic and anti-inflammatory agent [49], typically used to induce cell apoptosis [16]. RD detected lysosomal pH changes during apoptosis induced by dexamethasone (Fig. S17 and S19) in MCF-7 cells. The addition of dexamethasone decreased the fluorescence intensity in the cells in a time-dependent manner because of the increase in pH. However, without incubation with dexamethasone, the fluorescence intensity of RD showed no significant change even when the incubation time was prolonged (Fig. S18 and S19). Furthermore, apoptosis-related morphological changes were achieved 2.5 h after dexamethasone treatment (Fig. S17). This observation agrees with the literature [16, 50].

3.5 Imaging of ovarian tumour

Considering that most of the tumour tissues are partially acidic [27, 34, 51, 52], we focused on the detection of tumour in vivo using RD. Ovarian tumour model mice (7-week-old, 20-25 g) were bought from Dalian Medical College, China. Before animal imaging and analysis, the mice were starved for 12 h because of possible food fluorescence interference at the emission wavelength of the fluorescent dyes. Then, the ovarian tumour-bearing mouse was in-situ injected with RD (50 μL, 500 μM, in

DMSO) and observed using an in vivo imaging system. After injection of RD for 20 min, a strong fluorescence signal was detected in the tumour, and the fluorescence intensity became stronger along with the prolongation of time (Fig. 5).

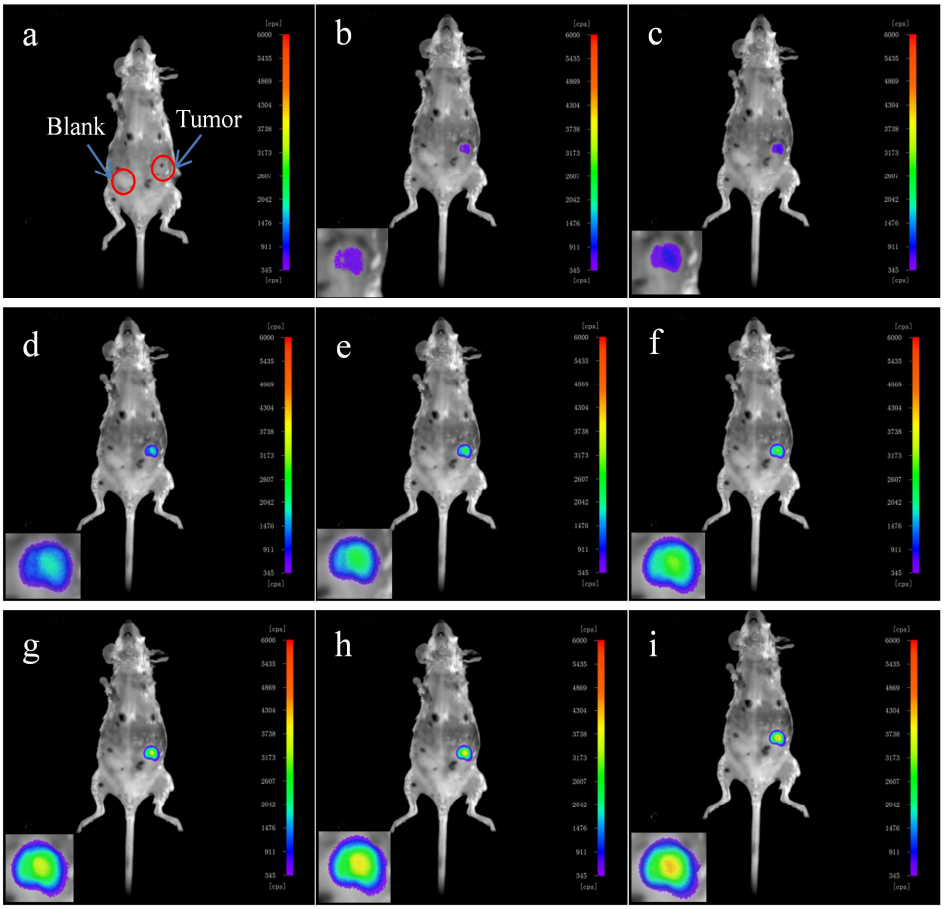

Fig. 5 Representative fluorescence images (pseudocolor) of mice given an in-situ injection of RD (50 μL, 500 μM, in DMSO) in tumour and blank respectively. (a) Blank, (b) in-situ injection of RD in tumour and blank for 10 min, (c) for 20 min, (d) for 40 min, (e) for 60 min, (f) for 80 min, (g) for 100 min, (h) for 120 min, (i) for 150 min. Images were taken with an excitation laser of 530 nm and an emission filter of 600 ± 20 nm. The inserted figure was the enlarged fluorescent position.

To provide further evidence, we dissected tumour and some organs from another group of ovarian tumour-bearing mice first, and then injected RD (50 μL, 100 μM, in DMSO) on the corresponding tumour and organs. As shown in Fig. 6, an exclusive emission signal was observed in the tumour 20 min after the injection. The fluorescent

signal in the tumour indicates that the acidity in ovarian tumour tissues is higher than that in normal tissues.

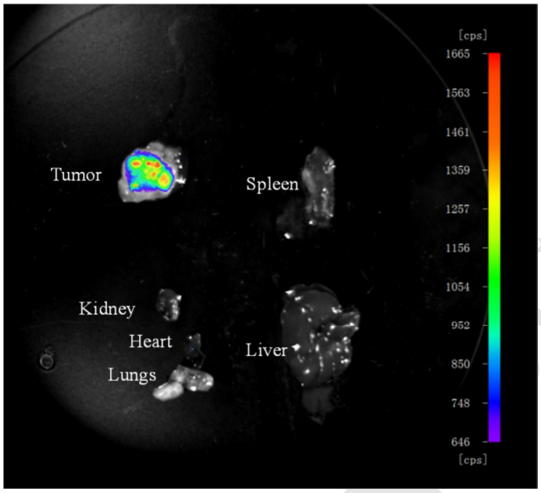

Fig. 6 Fluorescence images (pseudocolor) of tumour and organs excised from mice. Images were taken after injection 20 min with an excitation laser of 530 nm and an emission filter of 600 ± 20 nm.

3.6 Imaging in vivo mice

Hence, SPF mice starved 12 h were sacrificed. Then, the stomach and other organs were excised. As shown in Fig. S20, no fluorescence intensity was found for other organs. However, the fluorescence intensity in the stomach sharply increased after injection with RD for 30 min due to the pH of the stomach is less than 4 [53].

The Living mice administered with a skin-pop injection of RD (50 μL, 200 μM) and a mixture (100 μL) of phosphate buffer (10 mM) and EtOH (5/5, v/v) at pH 4.09 (Fig. 7) and 2.94 (Fig. S21) were also imaged using a Night OWL II LB 983 system equipped with an NC 100 CCD deep-cooled camera.

The fluorescence intensity became strongest after injection for 20 min (Fig. 7f), and then decreased along with time extension at pH 4.09 (Fig. 7g, h, i). The same trend can be observed in the case of pH 2.94 (Fig. S21), while the strongest fluorescent emission happened after injection for 15 min (Fig. S21e). The fluorescence intensity

was stronger and the response time was shorter at pH 2.94 than that at pH 4.09. In comparison, not any fluorescence can be observed in the corresponding blank control group. These results demonstrate that RD is an efficient fluorescent pH probe in vivo imaging.

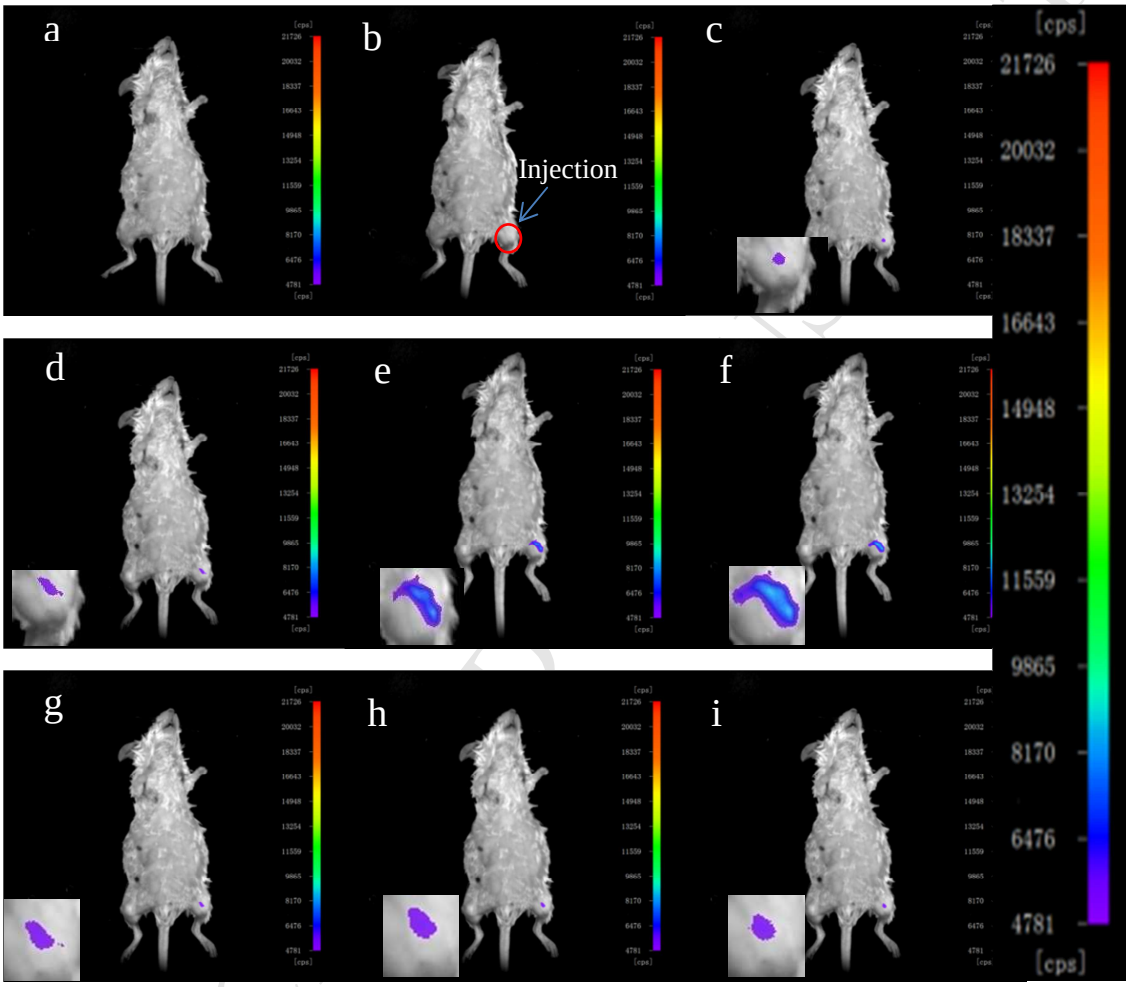

Fig. 7 Representative fluorescence images (pseudocolor) of mice given a skin-pop injection of RD (50 μL, 200 μM) and a mixture (100 μL) of phosphate buffer (pH 4.09, 10 mM) and EtOH (5/5, v/v). (a) Blank, (b) Skin-pop injection of a mixture of phosphate buffer (pH 4.09, 10 mM) and EtOH (5/5, v/v), (c) 10 min later, skin-pop injection of RD in the mouse in b for 5 min, (d) for 10 min, (e) for 15 min, (f) for 20 min, (g) for 25 min, (h) for 30 min, (i) for 40 min. Images were taken with an excitation laser of 530 nm and an emission filter of 600 ± 20 nm. The inserted figure was the enlarged fluorescent position.

4. Conclusions

In summary, a rhodamine B-based lysosomal pH probe termed RD with a pKa of 4.10 was developed. The probe exhibited high selectivity, good photostability and high reversible response to pH, as well as low cytotoxicity. RD can be an efficient pH probe for distinguishing cancer cells from normal cells and detecting tumours. The fluorescence signal in the ovarian tumour indicates that the acidity in tumor tissues is higher than that in normal tissues. Furthermore, RD performed well in complex biological systems, such as excised mouse stomach and living mice.

Acknowledgments

This work was financially supported by National Natural Science Foundation of China (Nos. 21272030, 21472016, 21306019, 21576042, 21421005).

References

[1] P. Boya, Lysosomal function and dysfunction: mechanism and disease, Antioxid. Redox Sign. 17 (2012) 766-774.

[2] L. Z. Chen, J. Li, Z. Z. Liu, Z. Ma, W. Zhang, L. P. Du, W. F. Xu, H. Fang and M. Y. Li, A novel pH "off–on" fluorescent probe for lysosome imaging, RSC Adv. 3 (2013) 13412-13416.

[3] G. M. Cooper and R. E. Hausman, The cell: amolecular approach, Sinauer Associates, Sunderland, MA, 2nd edn (2000) 725-730.

[4] J. L. Fan, C. Y. Lin, H. L. Li, P. Zhan, J. Y. Wang, S. Cui, M. M. Hua, G. H. Cheng and X. J. Peng, A ratiometric lysosomal pH chemosensor based on fluorescence resonance energy transfer, Dyes Pigment. 99 (2013) 620-626.

[5] M. M. Mohamed and B. F. Sloane, Near-infrared optical imaging of proteases in cancer, Nat. Rev. Cancer. 6 (2006) 764-775.

[6] M. I. D. Michelis, J. A. Raven and H. D. Jayasuriya, Measurement of cytoplasmic pH by the DMO technique in hydrodic tyonafricanum, J. Exp. Bot. 30 (1979) 681-695.

[7] G. A. Biagini, L. A. Knodler, K. J. Saliba, K. Kirk and M. R. Edwards, Na^+ - dependent pH regulation by the amitochondriate protozoan parasite Giardia intestinalis, J. Biol. Chem. 276 (2001) 29157-29162.

[8] D. J. Walker, S. J. Smith and A. J. Miller, Simultaneous measurement of intracellular pH and K^+ or NO^{3-}in barley root cells using triple-barreled, ion-selective microelectrodes, Plant Physiol. 108 (1995) 743-751.

[9] W. Roos, Ion mapping in plant cells–methods and applications in signal transduction research, Planta, 210 (2000) 347-370.

[10] W. Shi, X. Li, H. Ma, Fluorescent probes and nanoparticles for intracellular sensing of pH values, Methods Appl. Fluoresc. 2 (2014) 042001.

[11] J. Qi, D. Y. Liu, X. Y. Liu, S. Q. Guan, F. L. Shi, H. X. Chang, H. R. He and G. M. Yang, Fluorescent pH sensors for broad-range pH measurement based on a single fluorophore, Anal. Chem. 87 (2015) 5897-5904.

[12] M. H. Lee, N. Park, C. Yi, J. H. Han, J. H. Hong, K. P. Kim, D. H. Kang, J. L. Sessler, C. Kang and J. S. Kim, Mitochondria-immobilized pH-sensitive off–on fluorescent probe, J. Am. Chem. Soc. 136 (2014) 14136-14142.

[13] M. Y. Wu, K. Li , Y. H. Liu, K. K. Yu, Y. M. Xie, X. D. Zhou, X. Qi Yu, Mitochondria-targeted ratiometric fluorescent probe for real time monitoring of pH in living cells, Biomaterials, 53 (2015) 669-678.

[14] Y. C. Chen, C. C. Zhu, J. J. Cen, Y. Bai, W. J. He and Z. J. Guo, Ratiometric detection of pH fluctuation in mitochondria with a new fluorescein/cyanine hybrid sensor, Chem. Sci. 6 (2015) 3187-3194.

[15] A. R. Sarkar, C. H. Heo, L. Xu, H. W. Lee, H. Y. Si, J. W. Byun and H. M. Kim, A ratiometric two-photon probe for quantitative imaging of mitochondrial pH values, Chem. Sci. 7 (2016) 766-773.

[16] H. Zhu, J. L. Fan, Q. L. Xu, H. L. Li, J. Y. Wang, P. Gao and X. J. Peng, Imaging of lysosomal pH changes with a fluorescent sensor containing a novel lysosome-locating group, Chem. Commun. 48 (2012) 11766.

[17] K. K. Yu, K. Li, J. T. Hou, H. H. Qin, Y. M. Xie, C. H. Qian and X. Q. Yu, Rhodamine-based lysosome-targeted fluorescence probes: high pH sensitivity and their imaging application in living cells, RSC Adv. 4 (2014) 33975-33980.

[18] X. X. Zhao, X. P. Chen, Sh. L. Shen, D. P. Li, S. Zhou, Z. Q. Zhou, Y. H. Xiao, G. Xi, J. Y. Miao and B. X. Zhao, A novel pH probe based on a rhodamine–rhodamine platform, RSC Adv. 4 (2014) 50318-50324.

[19] S. L. Shen, X. P. Chen, X. F. Zhang, J. Y. Miao and B. X. Zhao, A rhodamine B-based lysosomal pH probe, J. Mater. Chem. B, 3 (2015) 919-925.

[20] J. T. Zhang, M. Yang, C. Li, N. Dorh, F. Xie, F. T. Luo, A. Tiwari and H. Y. Liu, Near-infrared fluorescent probes based on piperazine-functionalized BODIPY dyes for sensitive detection of lysosomal pH, J. Mater. Chem. B, 3 (2015) 2173-2184.

[21] W. W. Zhu, X. Y. Chai, B. G. Wang, Y. Zou, T. Wang, Q. G. Meng and Q. Y. Wu, Spiroboronate Si-rhodamine as a near-infrared probe for imaging lysosomes based on the reversible ring-opening process, Chem. Commun. 51 (2015) 9608-9611.

[22] Q. Q. Wang, L. Y. Zhou, L. P. Qiu, D. Q. Lu, Y. X. Wu and X. B. Zhang, An efficient ratiometric fluorescent probe for tracking dynamic changes in lysosomal pH, Analyst 140 (2015) 5563-5569.

[23] X. F. Zhang, T. Zhang, S. L. Shen, J. Y. Miao and B. X. Zhao, A ratiometric lysosomal pH probe based on the naphthalimide–rhodamine system, J. Mater. Chem. B, 3 (2015) 3260-3266.

[24] B. L. Dong, X. Z. Song, C. Wang, X. Q. Kong, Y. H. Tang and W. Y. Lin, Dual site-controlled and lysosome-targeted intramolecular charge transfer–photoinduced electron transfer–fluorescence resonance energy transfer fluorescent probe for monitoring pH changes in living cells, Anal. Chem., 88 (2016) 4085-4091.

[25] D. D. He, W. Liu, R. Sun, C. Fan, Y. J. Xu, and J. F. Ge, N-pyridineium-2-yl darrow red analogue: unique near-infrared lysosome-biomarker for the detection of cancer cells, Anal. Chem. 87 (2015) 1499-1502.

[26] J. Han and K. Burgess, Fluorescent indicators for intracellular pH, Chem. Rev. 110 (2010) 2709-2728.

[27] G. Helmlinger, A. Sckell, M. Dellian, N. S. Forbes and R. K. Jain, Acid production in glycolysis-impaired tumors provides new insights into tumor metabolism, Clin. Cancer Res. 8 **(**2002) 1284-1291.

[28] G. Helmlinger, F. Yuan, M. Dellian and R. K Jain, Interstitial pH and pO_2 gradients in solid tumors in vivo: high-resolution measurements reveal a lack of correlation, Nat. Med. 3 (1997) 177-182.

[29] C. M. Lemon, E. Karnas, X. X. Han, O. T. Bruns, T. J. Kempa, D. Fukumura, M. G. Bawendi, R. K. Jain, D. G. Duda and D. G. Nocera, Micelle-encapsulated quantum dot-porphyrin assemblies as in vivo two-photon oxygen sensors, J. Am. Chem. Soc. 137 (2015) 9832-9842.

[30] Y. Urano1, D. Asanuma, Y. Hama, Y. Koyama, T. Barrett, M. Kamiya, T. Nagano, T. Watanabe, A. Hasegawa, P. L. Choyke and H. Kobayashi, Selective molecular imaging of viable cancer cells with pH-activatable fluorescence probes, Nat. Med. 15 (2009) 104-109.

[31] M. Ogawa, N. Kosaka, C. A. S. Regino, M. Mitsunaga, P. L. Choyke and H. Kobayashi, High sensitivity detection of cancer in vivo using a dual-controlled activation fluorescent imaging

probe based on H-dimer formation and pH activation, Mol. Biosyst. 6 (2010) 888-893.

[32] M. V. Shirmanova, I. N. Druzhkova, M. M. Lukina, M. E. Matlashov, V. V. Belousov, L. B. Snopova, N. N. Prodanetz, V. V. Dudenkova, S. A. Lukyanov and E. V. Zagaynova, Intracellular pH imaging in cancer cells in vitro and tumors in vivo using the new genetically encoded sensor SypHer2, BBA-Gen. Subjects 1850 (2015) 1905-1911.

[33] H. Lee, W. Akers, K. Bhushan, S. Bloch, G. Sudlow, R. Tang and S. Achilefu, Near-infrared pH-activatable fluorescent probes for imaging primary and metastatic breast tumors, Bioconjugate Chem. 22 (2011) 777-784.

[34] R. C. Gilson, R. Tang, A. Som, C. Klajer, P. Sarder, G. P. Sudlow, W. J. Akers and S. Achilefu, Protonation and trapping of a small pH-sensitive near-infrared fluorescent molecule in the acidic tumor environment delineate diverse tumors in vivo, Mol. Pharmaceut. 12 (2015) 4237-4246.

[35] Z. Li, S. Q. Wu, J. H. Han and S. F. Han, Imaging of intracellular acidic compartments with a sensitive rhodamine based fluorogenic pH sensor, Analyst 136 (2011) 3698-3706.

[36] Britton H. T. K. and Robinson R. A., CXCVIII. —Universal buffer solutions and the dissociation constant of veronal. 1931. J. Chem. Soc. 1456-1462.

[37] E. L. Clennan, P. Dobrowolski and A. Greer, Reaction of singlet oxygen with thietane. A novel example of a self-catalyzed reaction which provides evidence for a thiadioxirane intermediate, J. Am. Chem. Soc. 117 (1995) 9800-9803.

[38] H. D. Li, Q. C. Yao, J. L. Fan, C. Hu, F. Xu, J. J. Du, J. Y. Wang and X. J. Peng, A fluorescent probe for ratiometric imaging of SO_2 derivatives in mitochondria of living cells, Ind. Eng. Chem. Res. 55 (2016) 1477-1483.

[39] H. N. Po and N. M. Senozan, The Henderson-Hasselbalch equation: its history and limitations, J. Chem. Educ. 78 (2001) 1499.

[40] H. D. Li, Q. C. Yao, J. L. Fan, J. J. Du, J. Y. Wang, X. J. Peng. An NIR fluorescent probe of uric HSA for renal diseases warning, Dyes and Pigments 133 (2016) 79-85.

[41] J. Tu, S. S. Sun and Y. Q. Xu, A novel self-assembled platform for the ratiometric fluorescence detection of spermine, Chem. Commun. 52 (2016)1040-1043.

[42] Y. Yuan, S. G. Sun, S. Liu, X. W. Song and X. J. Peng, Highly sensitive and selective turn-on fluorescent probes for Cu^{2+} based on rhodamine B, J. Mater. Chem. B, 3 (2015) 5261-5265.

[43] X. Q. Chen, T. Pradhan, F. Wang, J. S. Kim and J. Yoon, Fluorescent chemosensors based on spiroring-opening of xanthenes and related derivatives, Chem. Rev. 112 (2012)1910-1956.

[44] W. E. Ho, H. Y. Peh, T. K. Chan and W. S. Wong, Artemisinins: pharmacological actions beyond anti-malarial, Pharmacol. Ther. 142 (2014) 126-139.

[45] N. D. Yang, S. H. Tan, S. Ng, Y. Shi, J. Zhou, K. S. W. Tan, W. S. F. Wong and H. M. Shen, Artesunate induces cell death in human cancer cells via enhancing lysosomal function and lysosomal degradation of ferritin, J. Biol. Chem. 289 (2014) 33425-33441.

[46] L. Wang, Y. Xiao, W. M. Tian and L. Z. Deng, Activatable rotor for quantifying lysosomal viscosity in living cells, J. Am. Chem. Soc. 135 (2013) 2903-2906.

[47]X. L. Shi, G. J. Mao, X. B. Zhang, H. W. Liu, Y. J. Gong, Y. X. Wu, L. Y. Zhou, J. Zhang, W. H. Tan, Rhodamine-based fluorescent probe for direct bio-imaging of lysosomal pH changes, Talanta 130 (2014) 356-362.

[48] D. G. Smith, B. K. McMahon, R. Pal and D. Parker, Live cell imaging of lysosomal pH changes with pH responsive ratiometric lanthanide probes, Chem. Commun. 48 (2012) 8520-8522.

[49] H. Ohsugi, J. Hatsukawa, M. Takahara, M. Aizawa and N. Kanzawa, Real-time evaluation of the effects of dexamethasone on osteoblasts using dual labeling with fluorescent probes[C]//Key Engineering Materials, Trans. Tech. Publications 631 (2014) 379-383.

[50] K. Kagedal, M. Zhao, I. Svensson and U. T. Brunk, Sphingosine-induced apoptosis is dependent on lysosomal proteases, Biochem. J. 359 (2001) 335-343.

[51] W. X. Hou, X. Zhao, X. Q. Qian, F. Pan, C. L. Zhang, Y. M. Yang, J. M. Fuente and D. X. Cui, pH-Sensitive self-assembling nanoparticles for tumor near-infrared fluorescence imaging and chemo–photodynamic combination therapy, Nanoscale 8 (2016) 104-116.

[52] M. K. Gurka, D. Pender, P. Chuong, B. L. Fouts, A. Sobelov, M. W. McNally, M. Mezera, S. Y. Woo and L. R. McNally,Identification of pancreatic tumors in vivo with ligand-targeted, pH responsive mesoporous silica nanoparticles by multispectral optoacoustic tomography, J. Control. Release (2016).

[53] J. H. Seo, H. K. Park, J. S. Park, J. S. Yeom, J. Y. Lim, C. H. Park, H. O. Woo, H. S. Youn, J. S. Jun, G. H. Ko, S. C. Baik, W. K. Lee, M. J. Cho and K. H. Rhee,Association between gastric pH and helicobacter pylori infection in children, Pediatr. Gastr. Hepatol. Nutr. 18 (2015) 246-252.

Supplementary data (Fig. S1–S18)

A lysosomal probe for monitoring of pH in living cells and ovarian tumour

Bo Li[a,1], Guangbo Ge[b,1],Lanlan Wen[a,1],Ye Yuan[a], Ran Zhang[a], Xiaojun Peng[a], Fengyu Liu[a,*] and Shiguo Sun[c,*]

[a] *State Key Laboratory of Fine Chemicals, School of Chemistry, Dalian University of Technology, No. 2, Linggong Road, Ganjingzi District, 116023 Dalian, China.*
[b] *Dalian Institute of Chemical Physics, Chinese Academy of Sciences, Dalian 116023, China.*
[c] *Key Laboratory of Xinjiang Endemic Phytomedicine Resources, Ministry of Education, School of Pharmacy, Shihezi University, Shihezi 832000, China*
[1] *These authors contributed equally to this work.*

*Correspondence should be addressed to:
School of Chemistry, Dalian University of Technology,
No.2, Linggong Road, Ganjingzi District
Email: liufengyu@dlut.edu.cn
And Key Laboratory of Xinjiang Endemic Phytomedicine Resources, Ministry of Education,
School of Pharmacy, Shihezi University, Shihezi 832000, China
Phone: +86-29-87092226
Fax: +86-29-87082832
Email: sunsg@nwsuaf.edu.cn

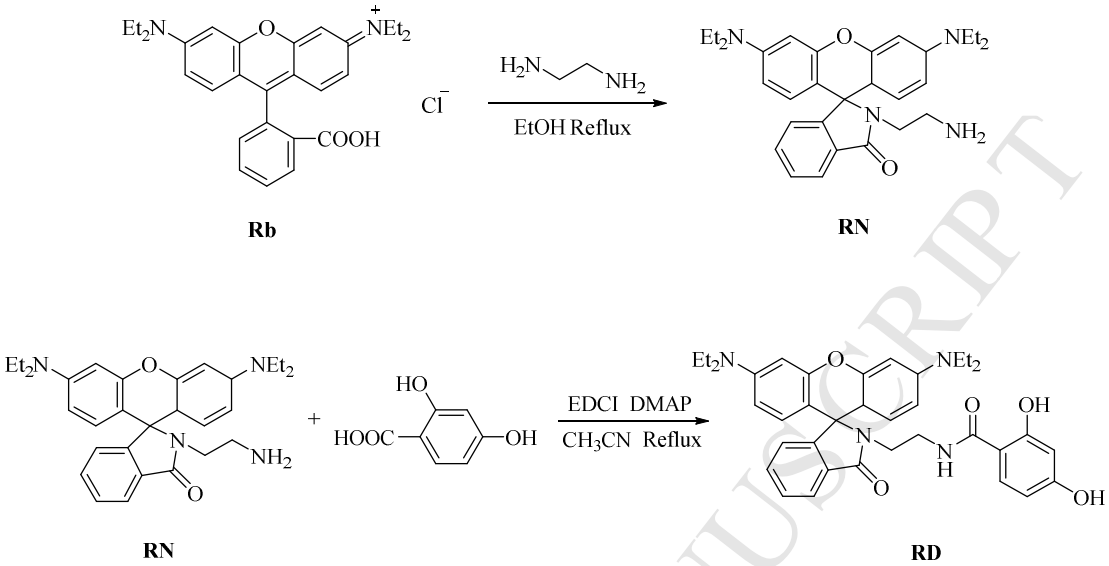

Scheme S1. Synthesis of compound RD

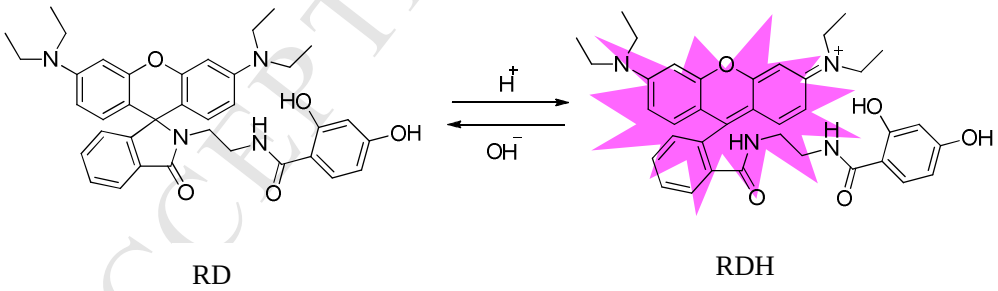

Scheme S2. Proposed Sensing Mechanism for H^+

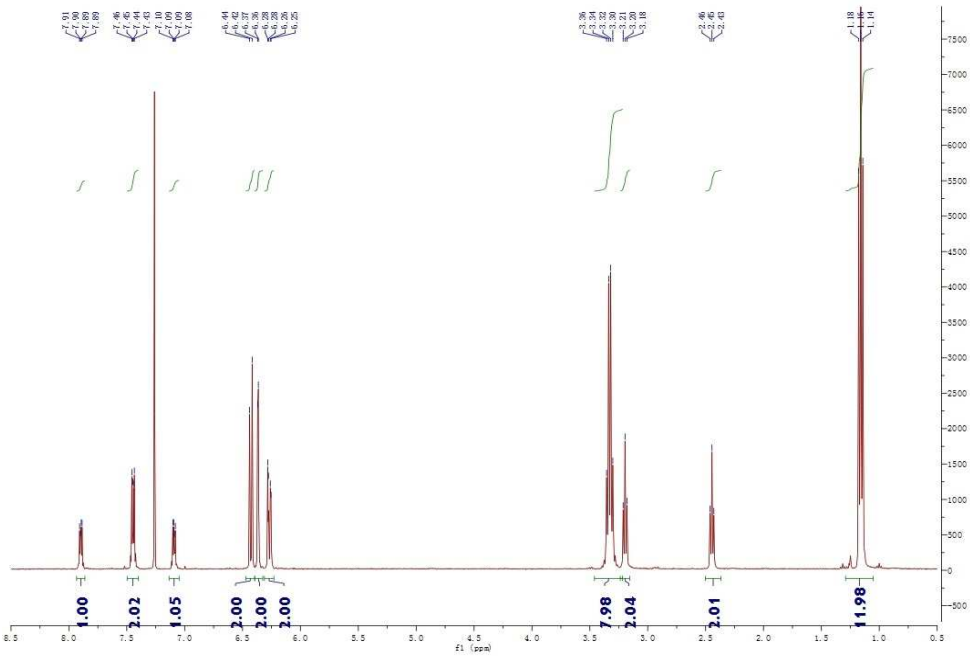

Fig. S1 ^{1}H NMR spectrum of R2 in $CDCl_3$

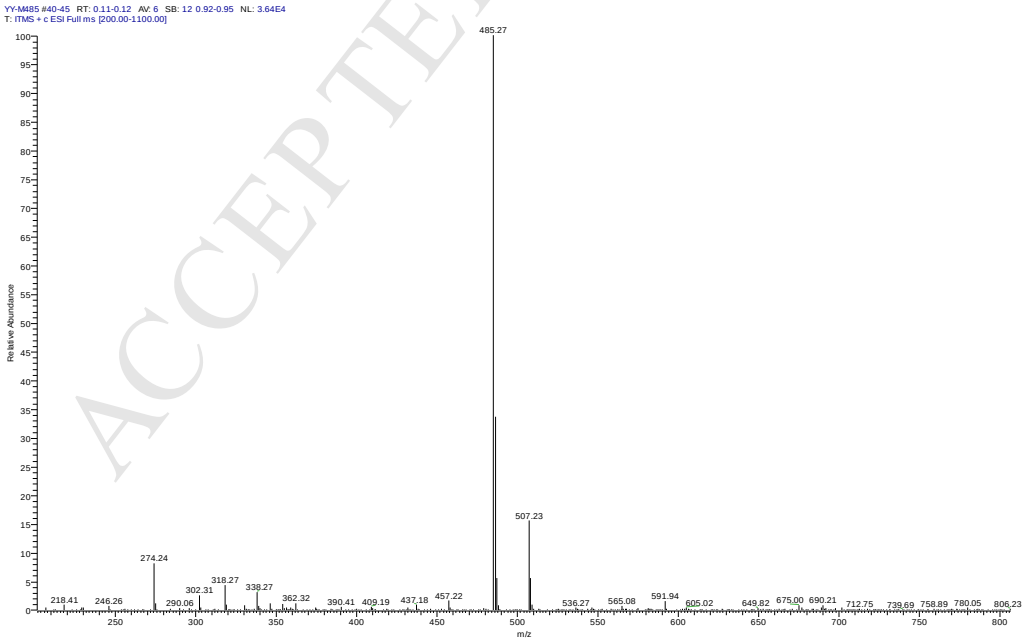

Fig. S2 MS spectrum of R2

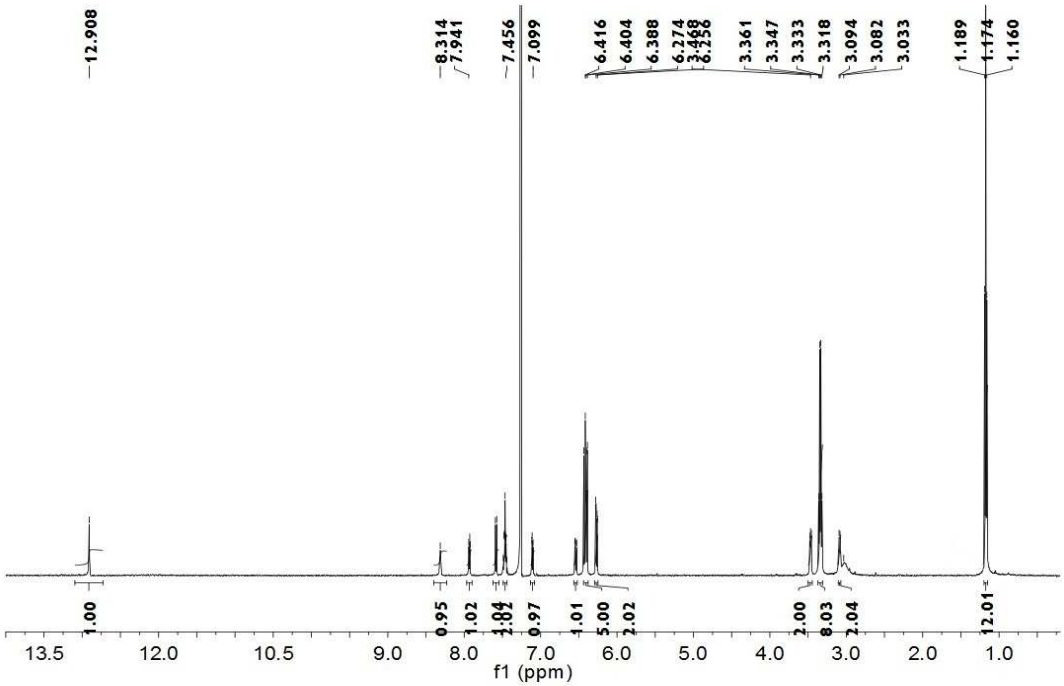

Fig. S3 ^{1}H NMR spectrum of RD in $CDCl_3$

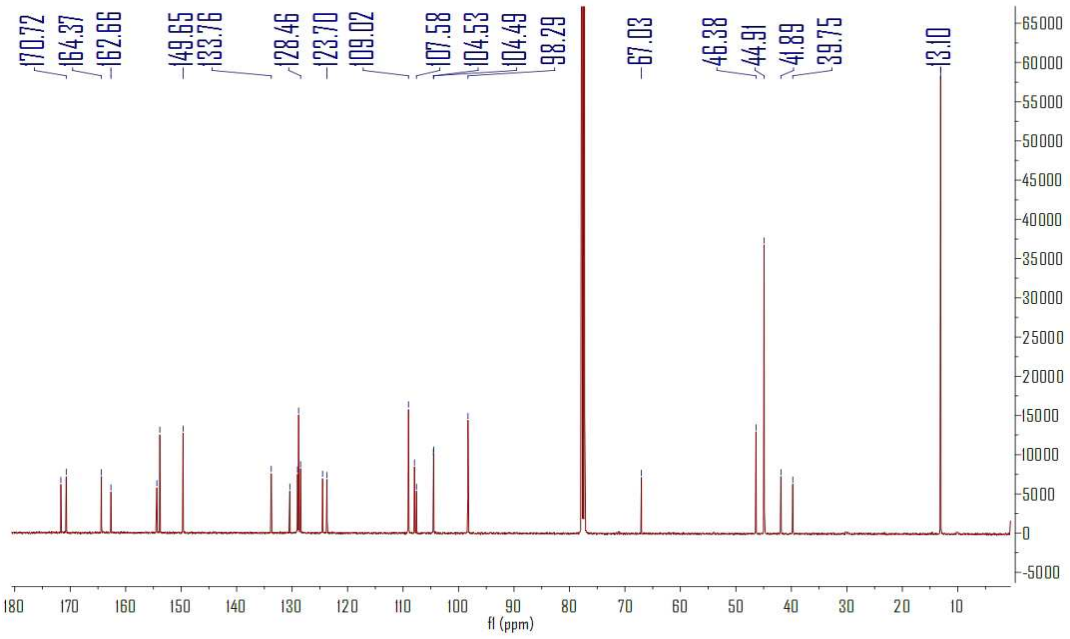

Fig. S4 ^{13}C NMR spectrum of RD in $CDCl_3$

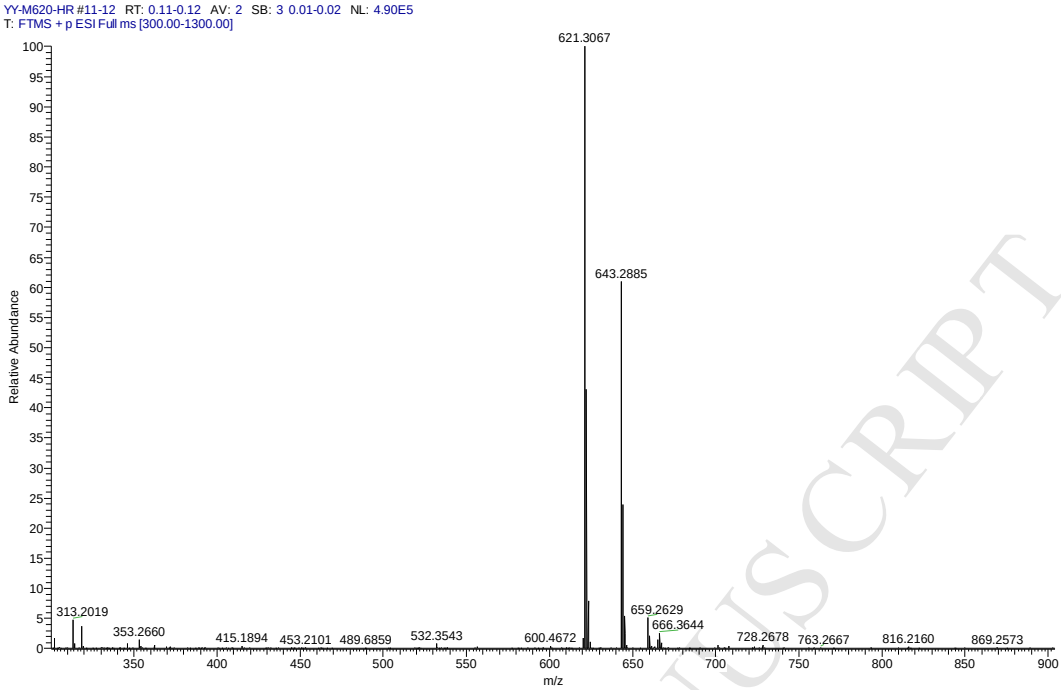

Fig. S5 HRMS spectrum of RD

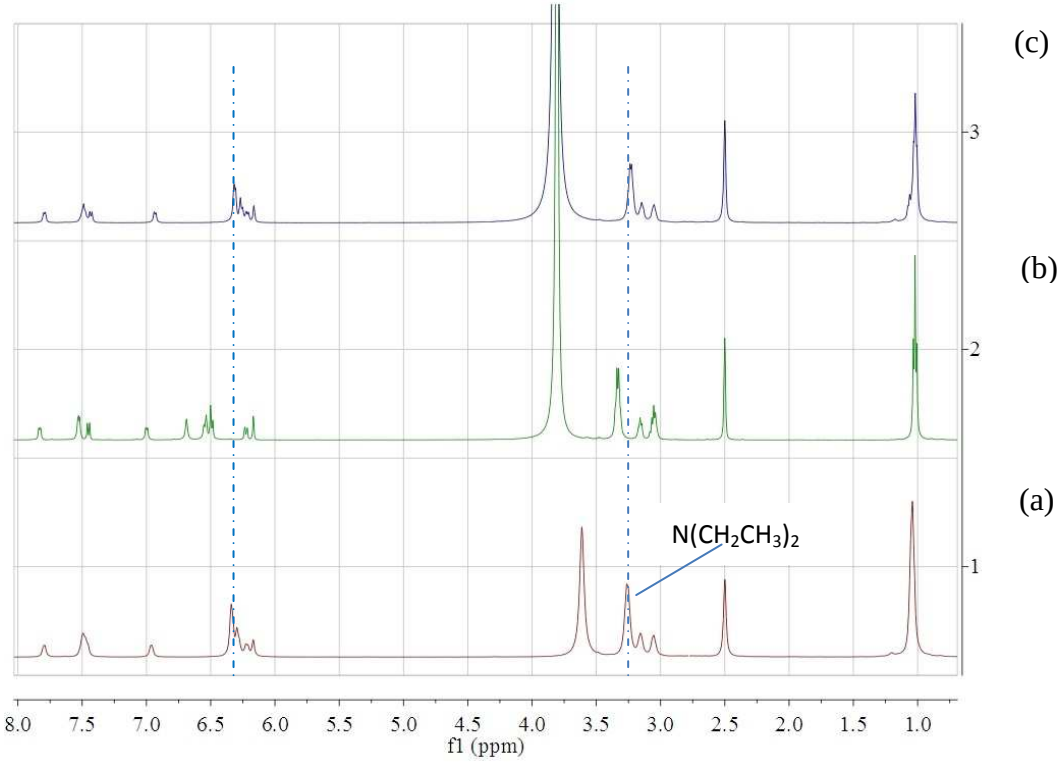

Fig. S6 Partial ^{1}H NMR spectra of (a) RD in DMSO-d_6/D_2O (9 : 1, v/v, adjusting pH to 7), (b) RD in DMSO-d_6/D_2O (9 : 1, v/v) in the presence of CF_3COOH (adjusting pH to 4), (c) RD inDMSO-d_6/D_2O (9 : 1, v/v) in the presence of CF_3COOH and then NaOH (adjusting pH to 7).The NaOH was dissolved in D_2O and made into 200 mM solution.

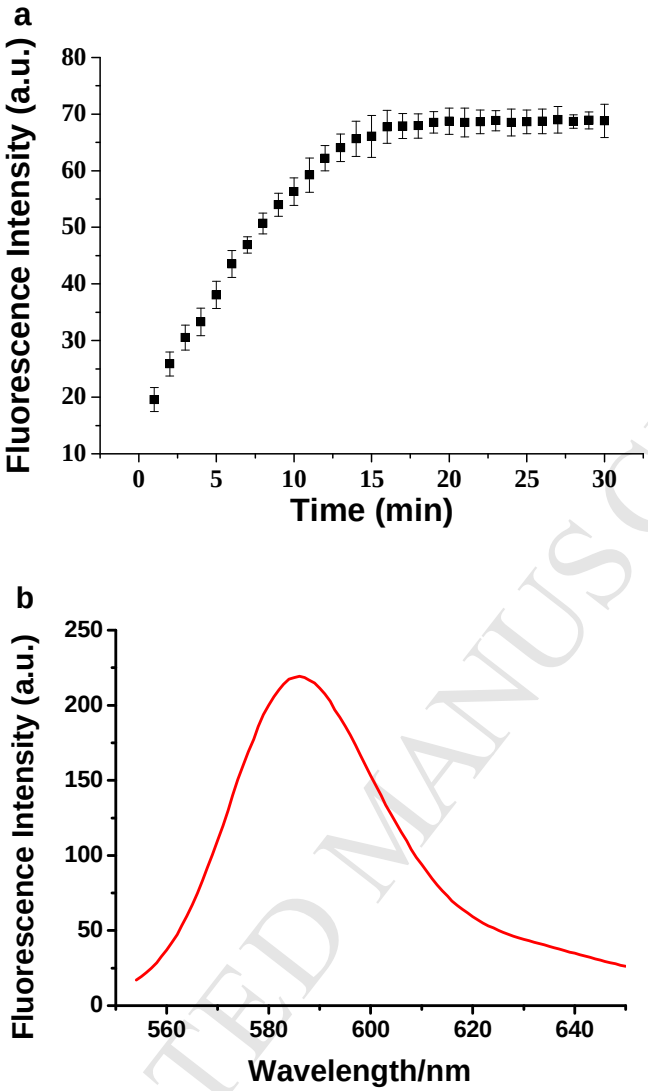

Fig. S7 (a) Time-dependent fluorescent intensities at 586 nm of RD (10 μM) in B-R-E solution when pH is 4.25. (b) Fluorescence spectra of RD (10 μM) in B-R-E solution with pH 3.26. (λ_{ex} = 540 nm).

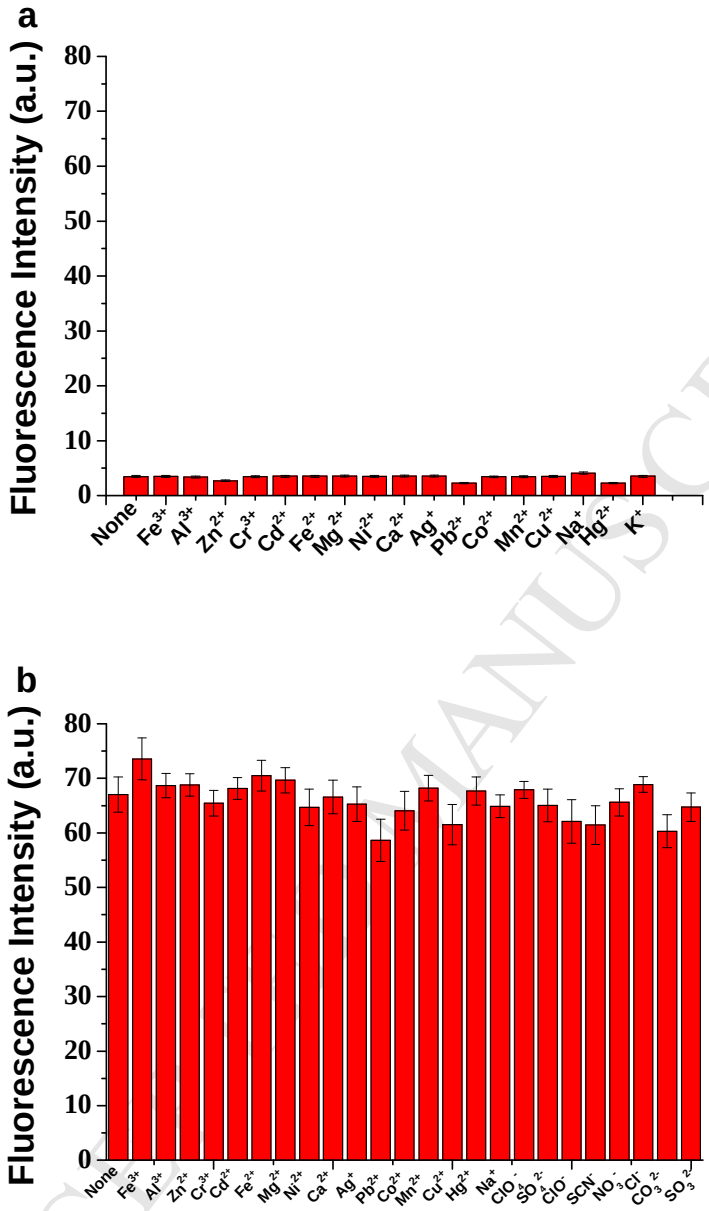

Fig. S8 Relative fluorescence intensity at 586 nm of RD (10 μM) in the presence of different ions in B-R-E solution, concentration of the other ions is 200 μM (a) pH = 7.02, (b) pH = 4.25 (λ_{ex} = 540 nm).

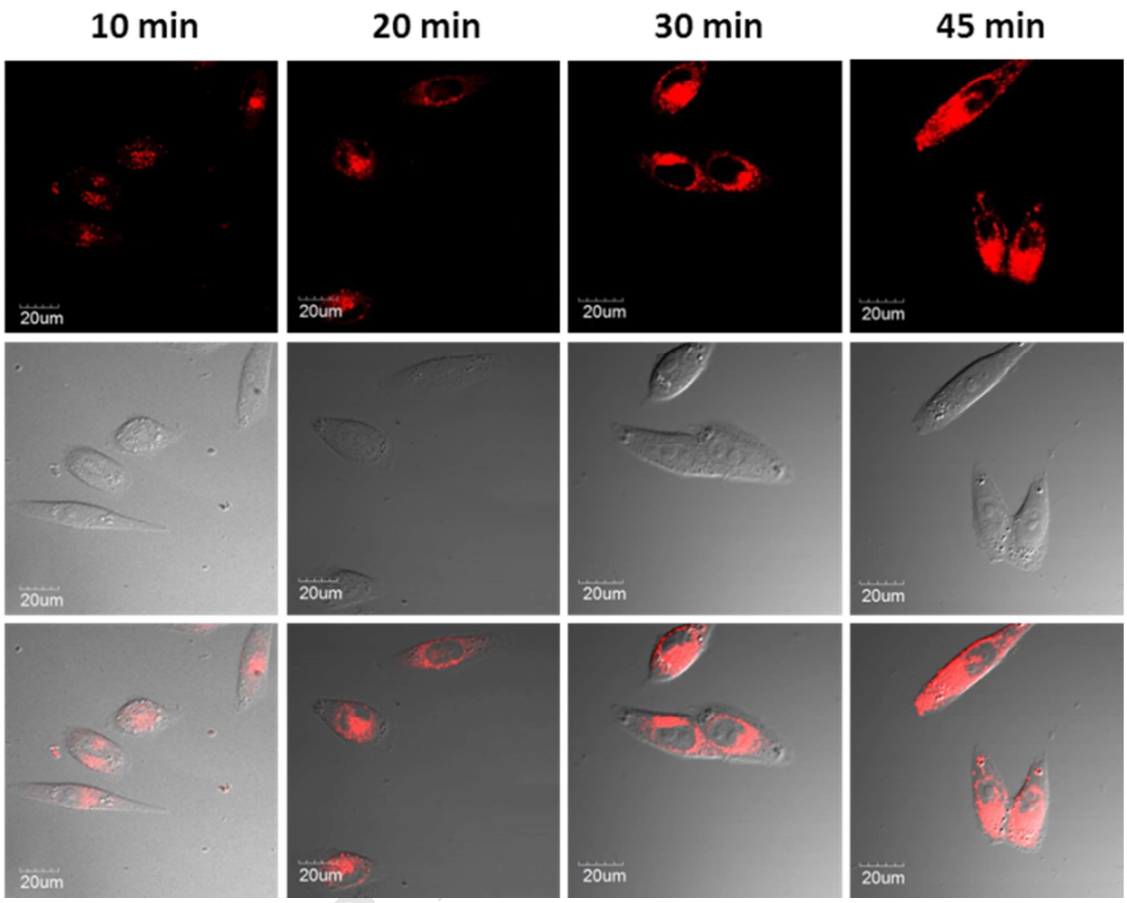

Fig. S9 Confocal fluorescence images of MCF-7 cells with RD (5 μM) after the cells were incubated for 10, 20, 30 and 45 min at 37 ºC under 5% CO_2, respectively. Scale bar: 20 μm, λ_{ex} = 559 nm, λ_{em} = 565-620 nm.

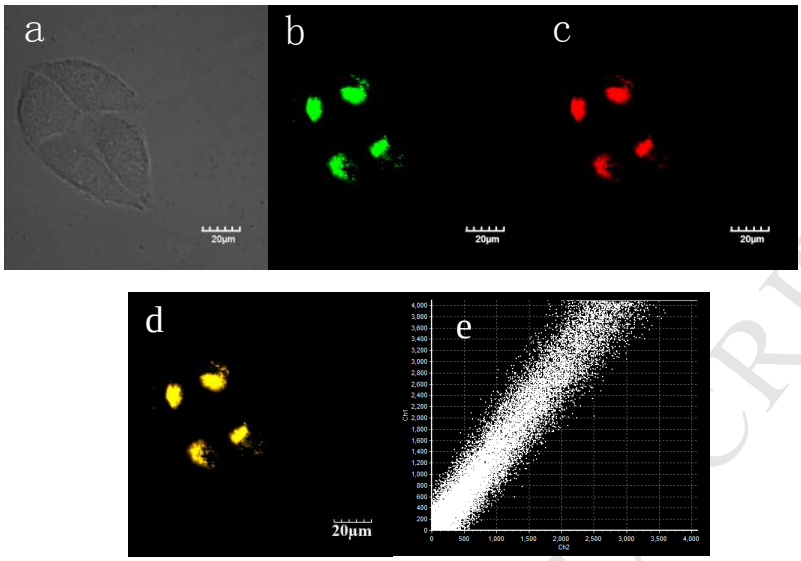

Fig. S10 Co-localization experiments of HeLa cells incubated with RD (5 μM) for 30 min and then incubated with Lyso Tracker Green (1.0 μM) for 10 min at 37 ºC under 5% CO_2. (a) Bright image, (b) Confocal image from LysoTracker Green on green channel (λ_{ex} = 488 nm), (c) Confocal image from RD on red channel (λ_{ex} = 559 nm), (d) Merged image of a, b and c, (e) Correlation plot of the intensities of RD and Lyso Tracker Green (Rr = 0.98).

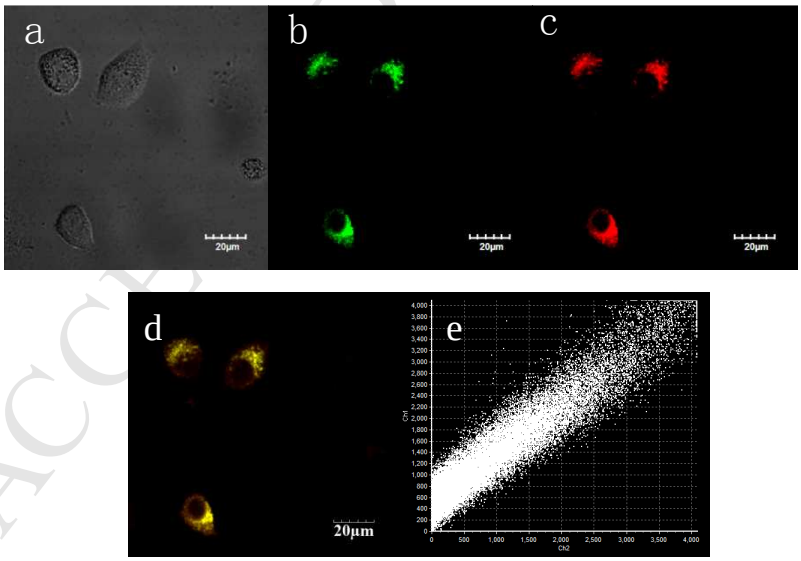

Fig. S11 Co-localization experiments of HepG-2 cells incubated with RD (5 μM) for 30 min and then incubated with LysoTracker Green (1.0 μM) for 10 min at 37 ºC under 5% CO_2. (a) Bright image, (b) Confocal image from Lyso Tracker Green on green channel (λ_{ex} = 488 nm), (c) Confocal image from RD on red channel (λ_{ex} = 559 nm), (d) Merged image of a, b and c,(e) Correlation plot of the intensities of RD and Lyso Tracker Green (Rr = 0.94).

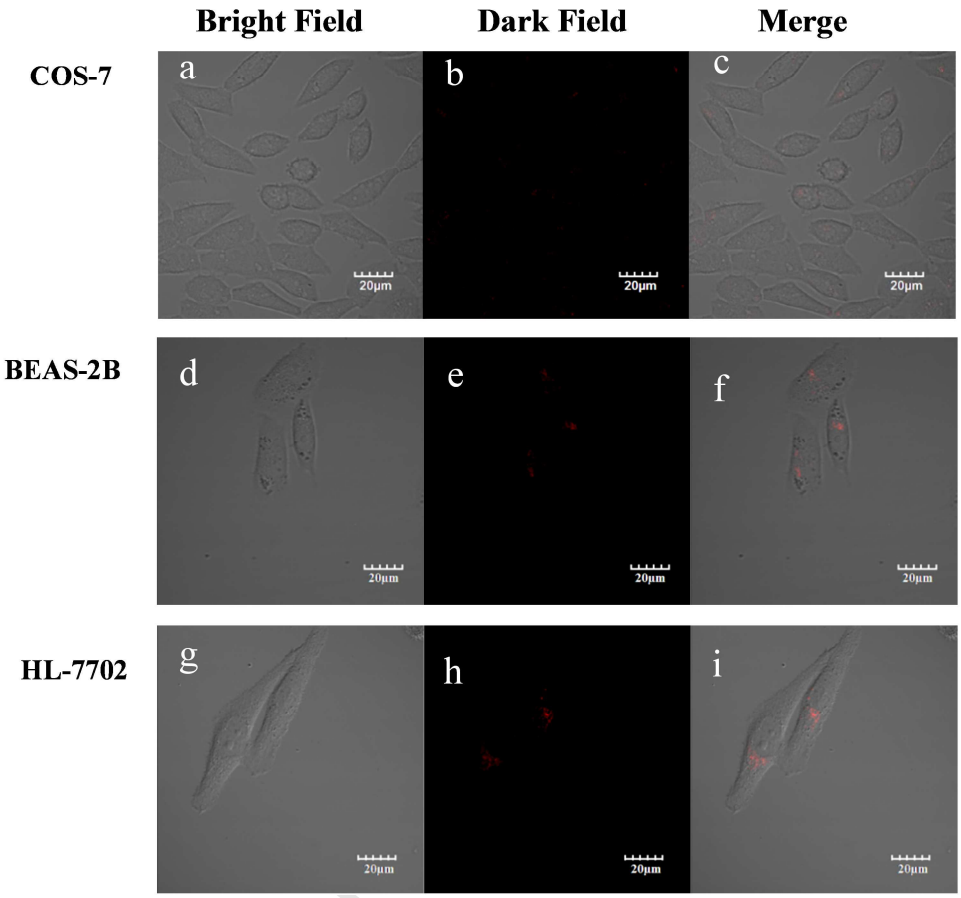

Fig. S12 Confocal fluorescence images of nomal cells with RD (5 μM) after the cells were incubated for 60 min at 37 ºC under 5% CO_2. (a-c) COS-7 cells, (d-f) BEAS-2B cells, (g-i) HL-7702 cells. Scale bar: 20 μm, λ_{ex} = 559 nm, λ_{em} = 565-620 nm.

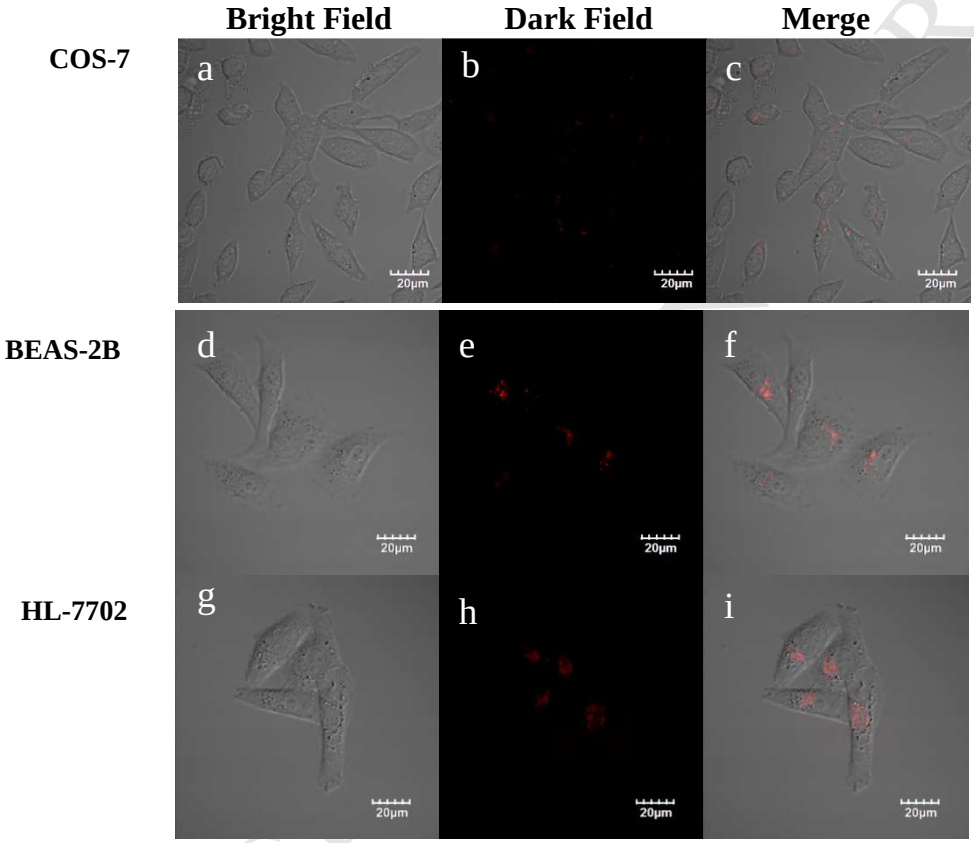

Fig. S13 Confocal fluorescence images of normal cells with RD (5 μM) after the cells were incubated for 120 min. (a-c) COS-7 cells, (d-f) BEAS-2B cells, (g-i) HL-7702 cells. Scale bar: 20 μm, λ_{ex} = 559 nm, λ_{em} = 565-620 nm.

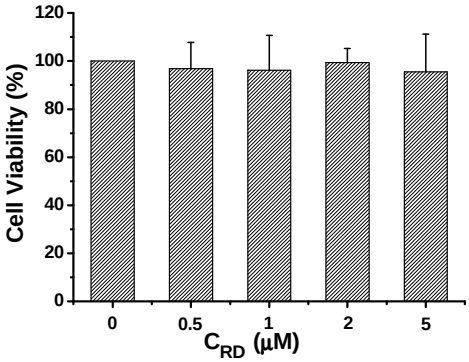

Fig. S14 Cytotoxicity studies of RD on HepG-2 cells by MTT analysis.

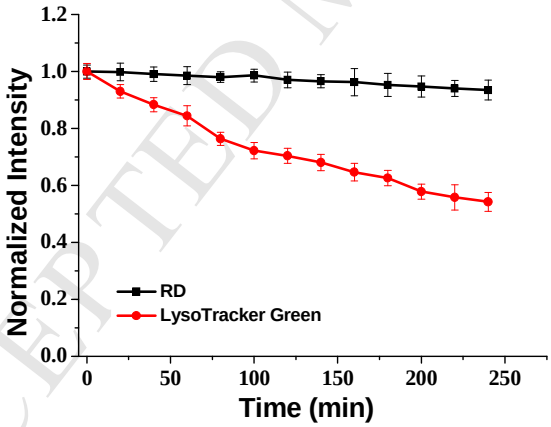

Fig. S15 Comparisons on the photostability of RD (10 μM) and Lyso Tracker Green (10 μM) in B-R-E solution (pH = 4.25) at room temperature. Irradiation under a 500 W halogen lamp for 4 h.

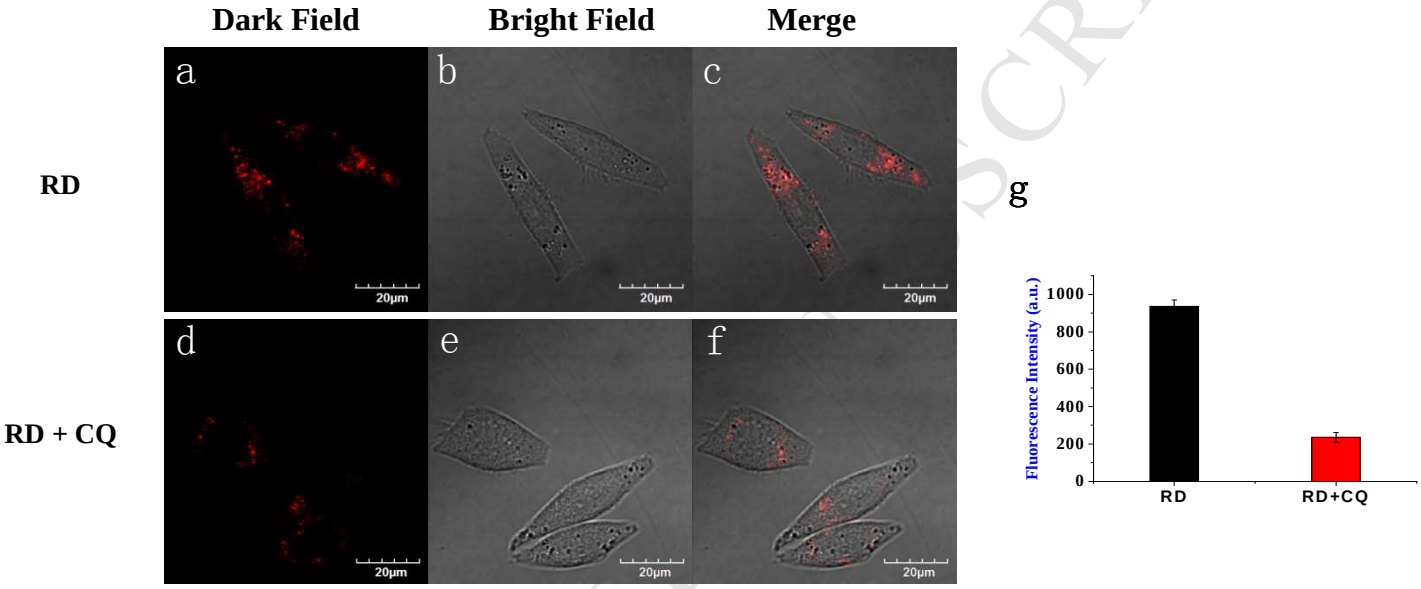

Fig. S16 Confocal image of RD (5.0 μM) incubated with 20 μM chloroquine in MCF-7 cells for 1 h. (a-c) incubated with RD in MCF-7 cells for 1.5 h, (d-f) incubated with RD for 0.5 h and then incubated with chloroquine for 1 h in MCF-7 cells, (g) Quantification of fluorescence intensity from RD and RD+CQ (chloroquine). Scale bar: 20 μm, λ_{ex}= 559 nm, λ_{em} = 565-620 nm.

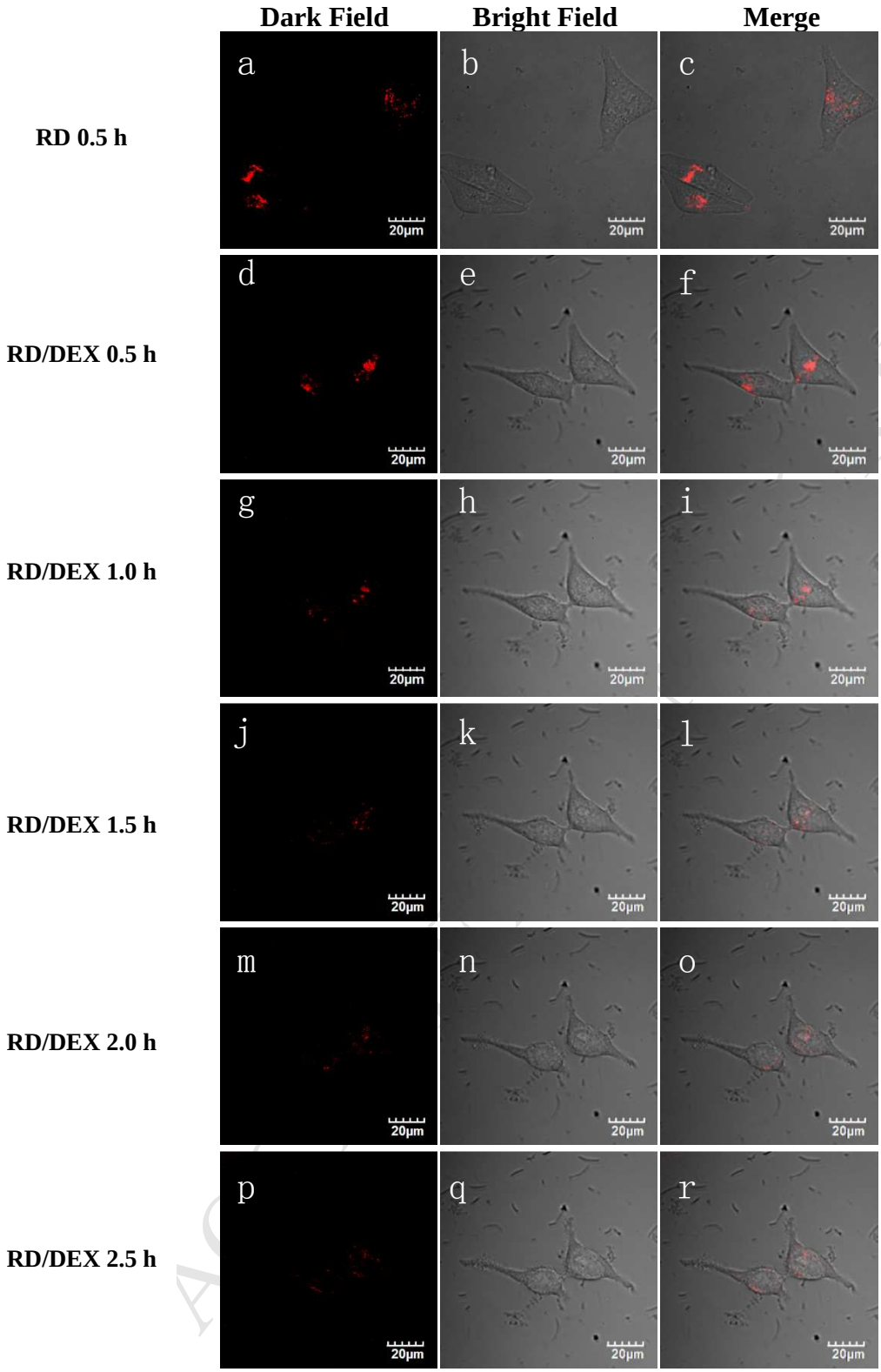

Fig. S17 Fluorescence images of RD (5 μM) in MCF-7 cells stimulated with dexamethasone. (a-c) Images of the stained cells before stimulation, (d-f) images of cells exposed to 100 μM dexamethasone for 0.5 h, (g-i, j-l, m-o, p-r) images of cells in (d-f) exposed to 100 μM dexamethasone for 1.0 h, 1.5 h, 2.0 h, 2.5 h respectively. Scale bar: 20 μm, λ_{ex} = 559 nm, λ_{em} = 565-620 nm.

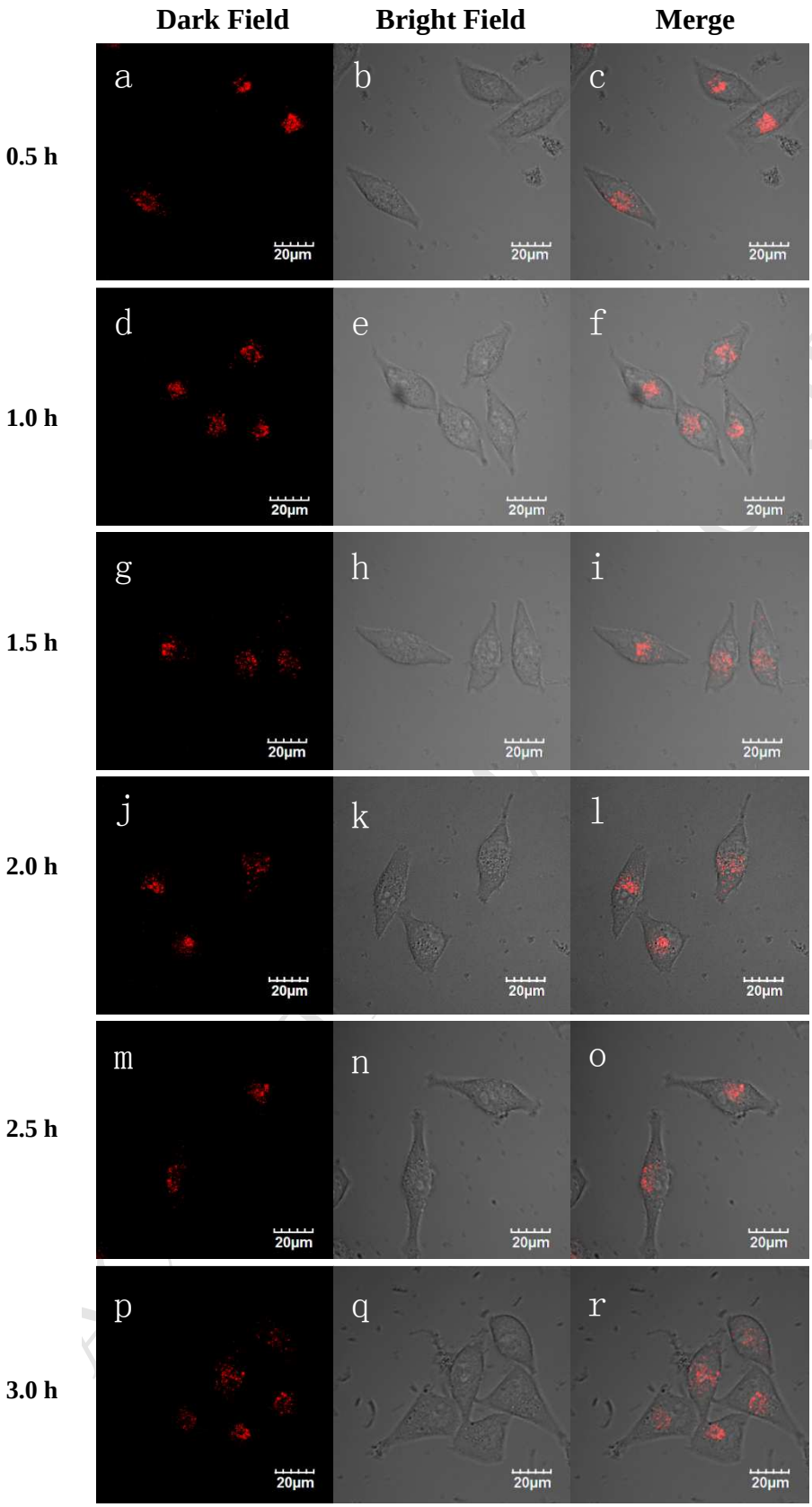

Fig. S18 Fluorescence images of RD (5 μM) in MCF-7 cells at different time. (a-c) 0.5 h, (d-f) 1.0 h, (g-i) 1.5 h, (j-l) 2.0 h, (m-o) 2.5 h, (p-r) 3.0 h. Scale bar: 20 μm, λ_{ex} = 559 nm, λ_{em} = 565-620 nm.

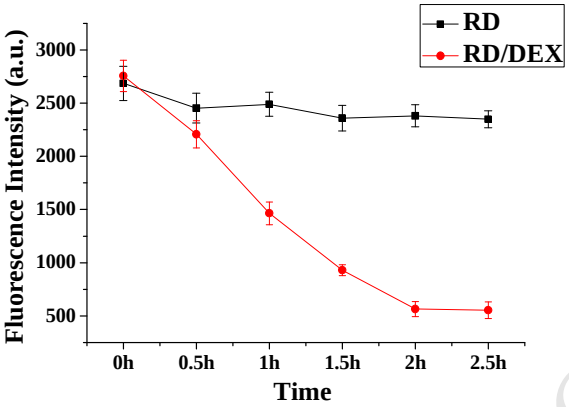

Fig. S19 Time dependent relative fluorescence intensity of RD and undergoing apoptotic death induced by dexamethasone (100 μM) in MCF-7 cells.

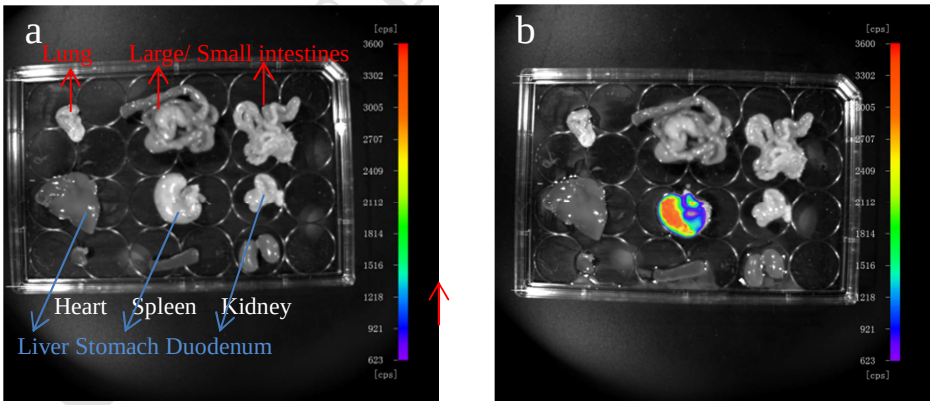

Fig. S20 Fluorescence images (pseudocolor) of organs excised from mice. (a) Blank, (b) Organs were given an injection of RD (50 μL, 100 μM, in DMSO). Images were taken with an excitation laser of 530 nm and an emission filter of 600 ± 20 nm.

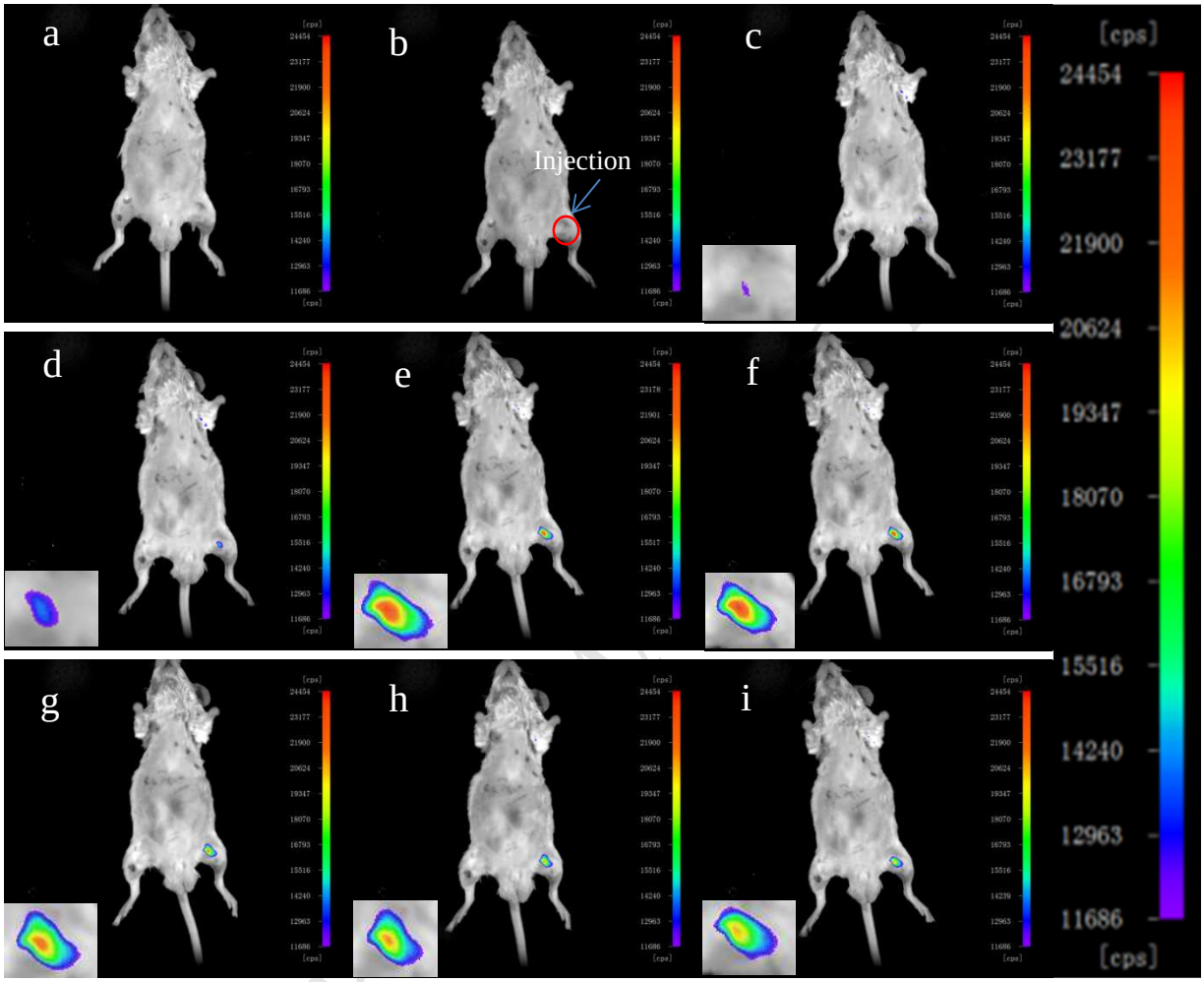

Fig. S21 Representative fluorescence images (pseudocolor) of mice given a skin-pop injection of RD (50 μL, 200 μM, in DMSO) and a mixture (100 μL) of phosphate buffer (pH 2.94, 10 mM) and EtOH (5/5, v/v). (a) Blank, (b) Skin-pop injection of a mixture of phosphate buffer (pH 2.94, 10 mM) and EtOH (5/5, v/v), (c) 10 min later, skin-pop injection of RD in the mouse in b for 2 min, (d) for 8 min, (e) for 15 min, (f) for 20 min, (g) for 25 min, (h) for 30 min, (i) for 40 min. Images were taken with an excitation laser of 530 nm and an emission filter of 600 ± 20 nm. The inserted figure was the enlarged fluorescent position.

Highlights:

- Probe RD can be employed to distinguish cancer cells from normal cells on the basis of fluorescence response.
- Performing well in the detection of lysosomal pH induced by artesunate, chloroquine and dexamethasone in cells.
- Distinguishing tumour tissues from normal tissues by intense fluorescence of RD in ovarian tumour.
- Working well in the imaging of ovarian tumour, excised mouse stomach and living mice under acidic stimulation.